Technical Report RSC-14

ANALYSIS AND EVALUATION OF A FORWARD VIEWING SCANNING RADAR SCATTEROMETER SYSTEM

by
Richard H Arnold

August 1970

supported by
National Aeronautics and Space Administration
NASA Grant ~~NsG-239-62~~ NGL-44-001-001

TEXAS A&M UNIVERSITY
REMOTE SENSING CENTER
COLLEGE STATION, TEXAS

ANALYSIS AND EVALUATION OF A FORWARD-VIEWING SCANNING RADAR SCATTEROMETER SYSTEM

A Thesis

by

RICHARD HARRISON ARNOLD

Submitted to the Graduate College of
Texas A&M University in
partial fulfillment of the requirement for the degree of
MASTER OF SCIENCE

August 1970

Major Subject Electrical Engineering

ABSTRACT

Analysis and Evaluation of a Forward-Viewing Scanning Radar Scatterometer System. (August 1970)

Richard Harrison Arnold, B S.,

University of Southwestern Louisiana

Directed by Dr. J. W. Rouse, Jr

A scatterometer is a radar system used to measure the radar cross-section of area extensive targets, particularly terrain As a part of the evolvement of this instrument, it has been proposed by a leading aerospace company that a scanning scatterometer be developed which would integrate for 0 2 seconds the returning signal from a terrain element defined by a minimum doppler frequency difference of 280 Hz. This system would provide measurements of the scattering coefficient of an area ±35 degrees transverse to the aircraft direction The purpose of this research effort was (1) to determine if the allowed integration time was sufficient for a given terrain element size for an accurate determination of the scattering coefficient, and if necessary, (2) to develop methods for improving the measurement accuracy without altering the basic scanning technique.

A scanning scatterometer is analyzed by system subassemblies transmission, reception, signal reduction

and logic, recording, and CRT display. Possible klystron transmission frequency drift problems and potential calibration problems are discussed. The calibration system is analyzed with respect to system operations An alternative system is presented and shown to be equal to or better than the proposed calibration system.

The accuracy of the scattering coefficient determination was shown to be directly related to the signal integration time and the terrain element size. The proposed integration time for the terrain element specified by the given doppler frequency difference was proven to be insufficient. Either an increase in the system's integration time or the element size is proven necessary to have sufficient accuracy.

An analysis of the possible use of frequency agility by the scatterometer system showed that definite advantages do exist. The use of frequency agility is shown to increase the accuracy of the scatterometer without increasing the integration time or the terrain element size. Further analysis involving defining a more exact analysis of the effect of frequency agility upon the accuracy of the scatterometer is suggested

ACKNOWLEDGEMENTS

I wish to thank Dr. J W Rouse, Jr., who is responsible for my introduction to the field of Remote Sensing and scatterometry, for his guidance towards my becoming an engineer. The assistance of the Ryan Aeronautical Co., especially Mr. Robert Chapman and Mr Corley Killion, was invaluable The financial support of the National Aeronautics and Space Administration under grant NsG 239-62 is sincerely appreciated.

A special acknowledgement is due my wife for the help, encouragement, and understanding she gave. I also wish to thank the secretaries Mrs James Ronald Bush and Mrs. Stanley Price.

TABLE OF CONTENTS

LIST OF TABLES

LIST OF FIGURES

CHAPTER I

INTRODUCTION

A scatterometer is a radar system used to measure the radar cross-section of area extensive targets, particularly terrain. As a part of the evolvement of this instrument, it has been proposed that a scanning scatterometer be developed [1] This system would provide measurements of the scattering coefficient of an area ±35 degrees transverse to the aircraft direction However, the engineering requirements for accomplishing the scanning operation demands a strict limitation on the time allowed for receiving the backscattered energy from each terrain element The purpose of this research effort was (1) to determine if the allowed integration time was sufficient, given a specific terrain element size, for an accurate determination of the scattering coefficient and, if necessary, (2) to develop methods for improving the measurement accuracy without altering the basic scanning technique

---

The citations on the following pages follow the style of the Proceedings of IEEE

The Scatterometer

Radar systems belong to the class of instruments termed remote sensors. These instruments are utilized to detect characteristics of objects from a distance in somewhat the same manner that the eye observes objects at a distance Remote sensors have been found to be useful, especially in earth resources studies, since they have the capability to observe objects under conditions where physical contact is impossible [2]

Radar systems are termed active sensors because they provide their own source of illumination This illumination is accomplished by transmitting electromagnetic waves Due to the nature of these waves, reflection from objects occurs and a portion of the reflected transmitted signal is directed towards the transmitter

Radar systems are capable of determining factors such as time delay, frequency difference, and power loss between transmission and reception From these three factors, certain characteristics of targets can be determined. Time difference can be used to determine the distance between the radar transmission source and the reflecting object. Frequency difference can be used for deteirmining relative velocity between the source and the object, or it can be used for spatial location using the

principle of the doppler frequency shift

Radar return is the result of signal reflection from an object Most objects, especially terrain surfaces, which radar systems are utilized to detect, have what is considered as "rough" surfaces Upon striking a rough surface, the radar signal will be dispersed in some pattern dependent upon the surface configuration For a large surface, such as the ground, many points within the surface constitute the object, or scatterer. For these large surfaces, radar return is subject to the scattering pattern of the sum of all the individual scatterers With a slight change in relative position between the radar source and the object composed of many individual scatterers, the scattering pattern may change considerably This causes the signal amplitude of the radar return to become random when motion occurs between the source and the object [3]

Parameters, other than the scattering pattern, affect radar return Some of these are angle of incidence, polarization, and transmission wavelength. These parameters are functions of the radar transmission Surface parameters affecting radar return are, in addition to roughness, electrical conductivity and permittivity All of these parameters will affect the power level of the radar return Those parameters which are functions of

radar transmission can be varied to observe power variation as a function of the parameter variation. Sometimes, these observations are useful in determining properties of the reflecting object One of these, variation of the angle of incidence versus a type of normalized power loss called the backscatter coefficient, is the main objective of the specific mode of radar system called the scatterometer.

A radar in the scatterometer mode measures the return power received from a ground area or object which scattered the signal transmitted by the radar. As stated, the primary objective of this radar mode is to obtain values of the radar backscatter coefficient, also called the differential scattering cross section, for a particular surface at a particular angle of incidence. As with other types of radar systems, the scatterometer can be designed to transmit and/or receive with different polarization schemes and to transmit at any particular microwave wavelength. Scatterometers are generally designed to determine the backscatter coefficient at several angles of incidence An ordinary radar system is capable of determining the backscatter coefficient for many types of objects but generally at only the particular angle of incidence at which the object is illuminated, and determining the angular, wavelength, or polar-

ızatıon dependence of the backscatter coefficient is not its primary objective. A scatterometer has become a distinct radar mode due to its peculiar type of operation

A surface is either rough or smooth relative to the incident wavelength A particular wavelength will determine the degree of roughness of the surface. This degree of roughness has the dominant effect upon the magnitude of the backscatter coefficient Since the degree of roughness will determine to a certain degree the scattered field pattern for terrain, the scattered field energy measured at any incidence or aspect angle is a function of the terrain roughness The large-scale terrain features will determine the magnitude of the backscatter coefficient for a small incidence angle, and for a large incidence angle, the small-scale structure determines the magnitude [4]

The overall effect of either the polarization of the incidence wave or the complex dielectric constant has not been adaquately determined For studies of specific materials, where their effect has been empirically determined, their utilization can prove effective [5]

Scatterometer data has proven to be useful in determining differences in sea ice types and sea state conditions The scatterometer has been shown capable of

determining the roughness variations in the homogeneous surfaces of the sea and ice. Scatterometer data taken from surfaces having non-homogeneous materials has been largely unsuccessful in determining the surface characteristics

Scatterometer data taken over the Arctic ice cap has provided backscatter coefficient versus incidence angle plots which have been used to distinguish young ice from old ice [6]. For the past several years, scatterometer data concerning sea reflectance has been collected. The assumption made to justify scatterometer utilization is that as the seas become more turbulent, the water surface becomes rougher. Investigations have shown that a correlation exists between sea state conditions and the backscatter coefficient [7]. However, recent work has also shown that there apparently exists a sea turbulence value above which the backscatter coefficient becomes useless for determining exact sea states [8]

Numerous investigations employing radar in the scatterometer mode are presently in progress. Texas A&M University [9], University of Kansas [10], Naval Research Laboratories [11], Ohio State University [12], Waterways Experiment Station [13], among others are attempting to further refine the capabilities and applications of this sensor.

The Scanning Scatterometer

Many laboratory experiments have been made in order to obtain backscatter coefficient versus incidence angle plots for various soils, road types, and crop types Some of this data has been collected to provide a catalog standard for scatterometer data analysis [14]

Present airborne scatterometer systems view beneath the aircraft within a very narrow beamwidth For example, the NASA MSC scatterometer views beneath the aircraft within a ±1 5 degree beamwidth This drastically limits the terrain coverage per flight. Therefore, a more efficient viewing scatterometer, one which is capable of viewing more surface area per flight, is desirable Such a scatterometer is the proposed scanning scatterometer

The scanning scatterometer is designed to view ground area transverse to the aircraft as well as along the flight direction. This is accomplished partially by sweeping the scatterometer antenna pattern coverage transverse to the aircraft direction Basic to the scanning scatterometer is the use of the doppler frequency shift to help delineate the specific ground location to be viewed No known sufficient quantitative analysis of the ability of the scanning scatterometer to

effectively determine backscatter coefficient values has been made. This effectiveness is directly related to the use of the doppler frequency shift. Therefore, such an analysis will be partially concerned with the effect of using the doppler frequency shift This research develops this analysis for a specific scanning scatterometer to be described in Chapter II.

Summary

In this document, a scanning scatterometer system is described using block diagram type notation. The system is presented in sections associated with the scatterometer subassemblies, transmission, reception, signal reduction and logic, recording, and CRT display, in Chapter II. This Chapter is the basis for subsequent examinations in Chapters III and IV.

A theoretical analysis of the scanning scatterometer system was performed in Chapter III with respect to the determinance of the backscatter coefficient. Due to the stochastic nature of a backscattered signal, this analysis was conducted using probability theory. The signal power spectrum is traced through the signal reduction section The resultant signal spectrum after half-wave linear detection is computed. The number of independent samples available during the integration period was de-

termined From this information, the accuracy of the ability of the scatterometer to determine the backscatter coefficient was calculated by using the average power variance and the average voltage squared variance

The advantages of implementing frequency agility on future scanning scatterometer systems are determined in Chapter IV with respect to previous studies [15] concerning frequency jumping radar systems The loss of accuracy in determining the backscatter coefficient by frequency agility was weighed against the possibility of increasing the number of independent samples available during the integration time The results show that frequency agility implementation is advantageous from the standpoint of increasing the accuracy of the backscatter coefficient determinations

A summary of the study and recommendations for further work is presented in Chapter V. Further work is recommended to determine the full potential of using frequency agility on future scatterometer systems.

CHAPTER II

SYSTEM

Transmission

Transmission, as with any radar system, is described in terms of transmitting and receiving periods, signal features, and antenna pattern This system is designed with the intent to incorporate two altitude ranges, thus requiring dual transmission modes. Therefore, transmission and power specifications will be discussed separately from the antenna design and pattern.

The transmitted frequency is the interrupted continuous wave (ICW) type The system operates at 13 3 GHz using a klystron power output of ten watts minimum The pulse repetition frequency (PRF) of this signal is a function of aircraft velocity and altitude in each altitude range. This is also the case for the transmitting and receiving periods (see Fig. II-1) [16]

Since ground return is desired from points up to 50 degrees from the aircraft nadir, reception time must at least equal twice the time for a signal to be transmitted to the furthest point Therefore,

$$T_r = \frac{2 h_{max}}{c \cos\theta} \qquad (2\text{-}1)$$

Knowing the transmitting and receiving periods, the pulse repetition frequency is found to be

$$\frac{1}{PRF} = T_t + T_r + 2T_d$$

Substituting the value for maximum receiving time

$$\frac{1}{PRF} = \frac{c(T_t + 2T_d)\cos\theta + 2h_{max}}{c\cos\theta} \qquad (2\text{-}2)$$

where c = speed of light
θ = incidence angle
T_t = transmitting time
T_d = time delay between transmission and reception
h_{max} = maximum aircraft height

This PRF is subjected to a lower limit due to the system. The transmitted signal is subjected to a frequency shift upon striking the ground This doppler frequency shift (f_d) is used in the system to delineate ground area, hence by the sampling theorem, the minimum PRF is

$$PRF_{min} \geq 2f_{d\,max} \qquad (2\text{-}3)$$

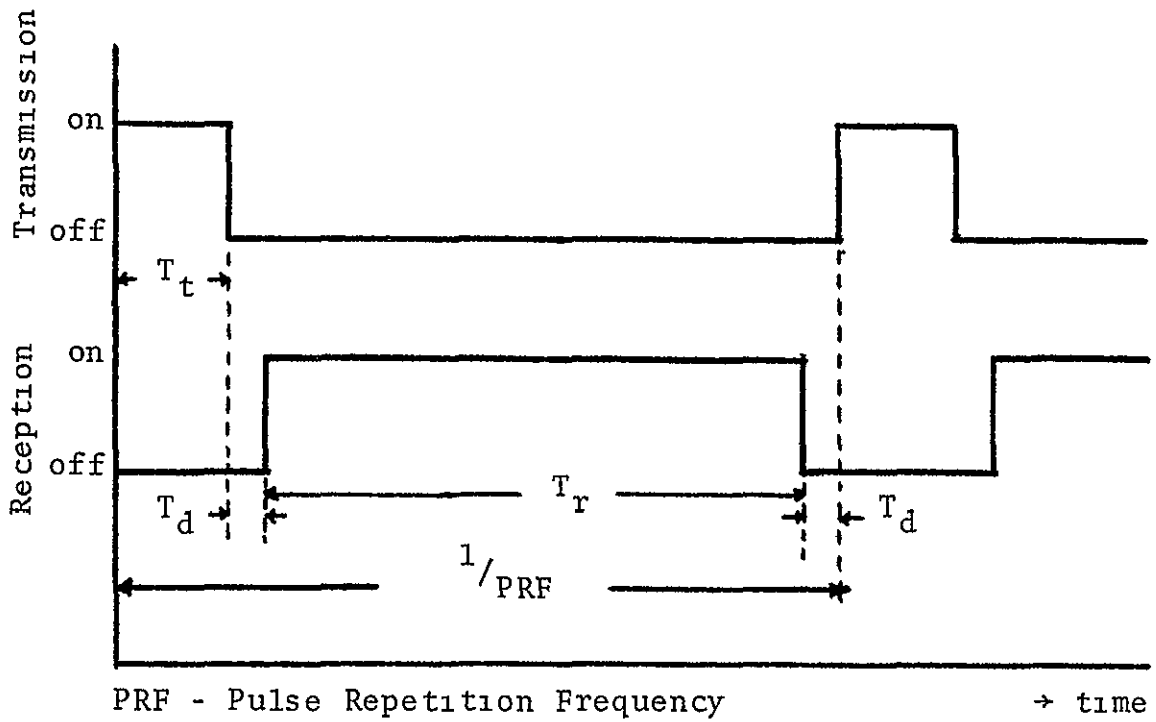

FIG. II-1 PULSE REPETITION FREQUENCY DIAGRAM

For a view at a constant angle of incidence, a maximum f_d occurs at the ground area in the flight direction. Doppler frequency shift along this line is defined as

$$f_d = \frac{2v}{\lambda} \sin\theta = \frac{2vf}{c} \sin\theta \qquad (2\text{-}4)$$

Therefore, taking theta maximum as 50 degrees, and maximum velocity as 300 knots (154 meters per second)

$$f_{d\,max} = \frac{2(154)(13.3\times10^9)}{3\times10^8} \sin\theta = 10.47\ KHz \qquad (2\text{-}5)$$

and $$PRF_{min} > 2f_{d\,max} = 20.94 KHz \qquad (2\text{-}6)$$

where v = aircraft velocity
f = transmitted frequency
λ = transmitted wavelength
c = speed of light

Two altitude ranges are selected of which the minimums were 2,000 ft. and 5,000 ft Using a time of one microsecond for T_d, two transmission modes are obtained and shown in Table II-1.

The signal is continuous when emitted from the klystron. Pulse modulation is accomplished by the use of a duplexing switch, the maximum switching rate being 45 KHz.

Altitude	Transmitting Pulse	Pulse Rate Frequency
2,000 - 5,000 ft.	4.08 µsec	45 KHz
4,000 - 10,000 ft.	8.16 µsec.	22.5 KHz

TABLE II-1 TRANSMISSION MODES

The scatterometer uses a klystron in the transmission section (see Fig. II-2) The klystron is a high frequency signal generator and amplifier. The reflex klystron or a multicavity klystron with feedback is most commonly used for this purpose Klystrons, being compact, efficient at high frequencies, and of simple construction, are utilized in place of tubes. Tubes generally have relatively large electrodes and long lead wires which create capacitance and inductances too large for a microwave resonant circuit Also, the electron transit angle is large for tubes at microwave frequencies causing an output delay in the tube (i e. increased transadmittance). To minimize these effects, tubes can be miniturized, but this limits power-handling capabilities [17].

The klystron circumvents these problems. First of all, it can be of compact construction. Second, it utilizes cavities for the microwave resonant frequency, and third, the electron transit angle can be minimized

The klystron (Fig. II-3) is basically a tube with cavities operating on the principle of electron velocity modulation. Amplification occurs by feeding a signal into the input cavity, called the buncher At any one time, the voltage across the buncher gap will be $v_1 = V_1 \sin \gamma t$, where V_1 is the input voltage and γ is the signal frequency Electrons passing the gap when $v_1 = V_1$ will

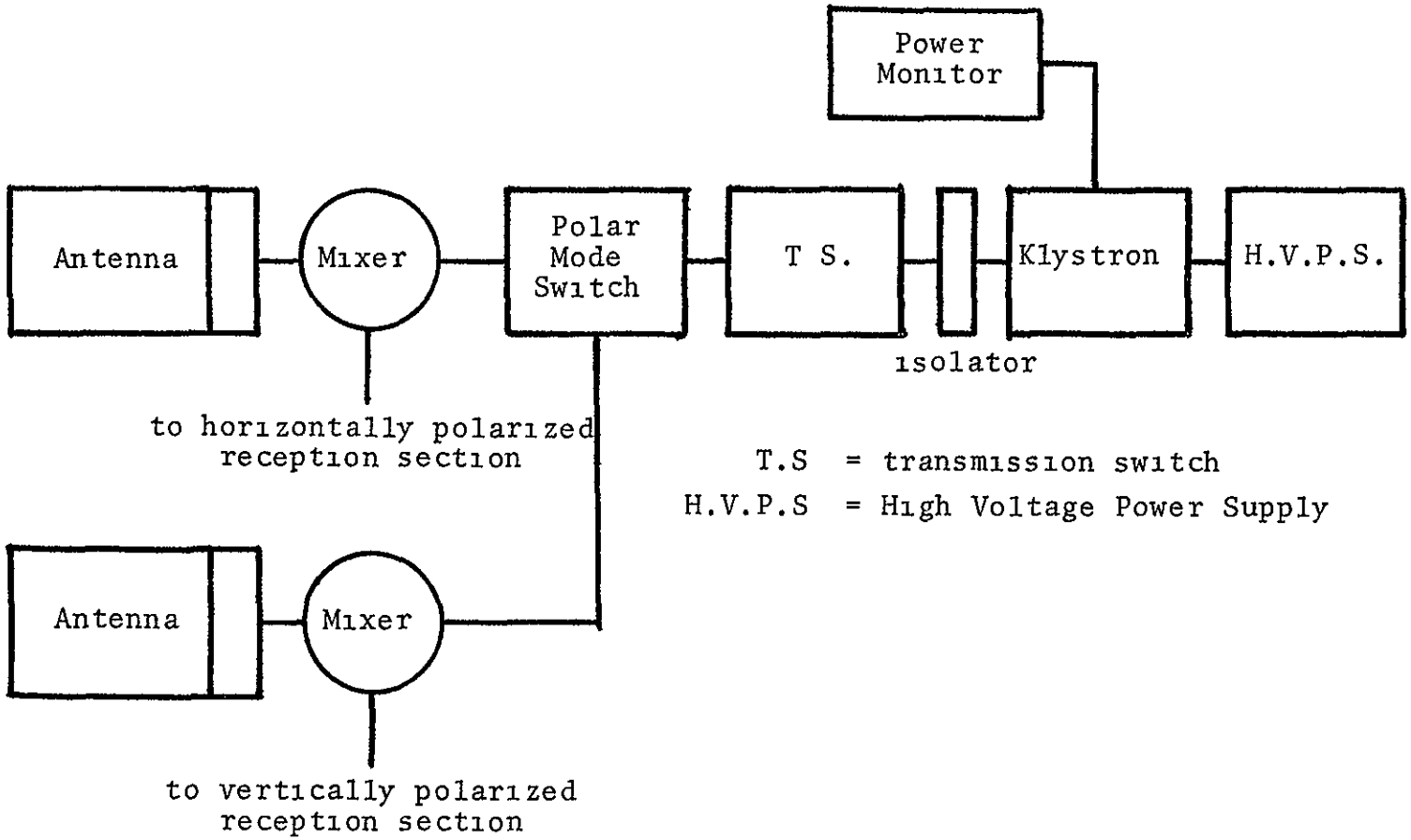

FIG II-2 TRANSMISSION SECTION

travel slower than electrons passing the gap when $v_1 = 0$ Electrons will travel their fastest when $v_1 = V_1$ Thus, the electrons are velocity modulated by the voltage across the buncher gap

These electrons are emitted from a cathode and focused into a beam by the electron gun. The cavities are at a positive potential for beam acceleration and not for electron attraction purposes After the electrons are velocity modulated by the initial cavity, they tend to bunch up in the drift space Electrons accelerated during the high voltage period overtake those slowed by the previous low voltage period, thus causing the bunching effect. They then pass through the catcher cavity and collide with the collector

The catcher cavity, or output cavity is placed such that its gap is at the place of maximum bunching Here, power is extracted from the bunched electrons The energy received from the bunched electrons is generally many times greater than that required to velocity-modulate the electron beam. Thus, amplification occurs Oscillation can be obtained very easily by coupling the buncher and catcher with a feedback circuit. The frequency will be the resonance frequency of the oscillator having a no-load condition

In multicavity klystrons, several buncher cavities are used. Proper adjustment of the phase and magnitude of the waves in these bunchers produces a very tightly bunched electron beam. This additional bunching increases the output gain.

A reflex klystron (Fig. II-4) utilizes only one cavity to achieve oscillation. Electrons are emitted by the cathode and are velocity modulated when initially passing through the cavity grids These grids are held at a positive d-c potential with respect to the cathode and will have the voltage operation shown in Fig. II-5.

By proper adjustment of the beam acceleration and repeller voltages, the variation of voltage on the grids, caused by initial oscillation, will cause resonance. The electrons are repelled by the highly negative reflector and pass back through the grid gap. If the bunched electrons are slowed down by the gap-voltage cycle, their energy is applied to the oscillation.

The duplexer switches are devices which switch an antenna either to the transmitter or receiver. These switches are pieces of ferrite strips whose impedance is controlled by an externally applied d-c magnetic field Signals create magnetic fields which, using the non-isotropic property of ferrite, create low loss transmission in one direction and almost total power absorp-

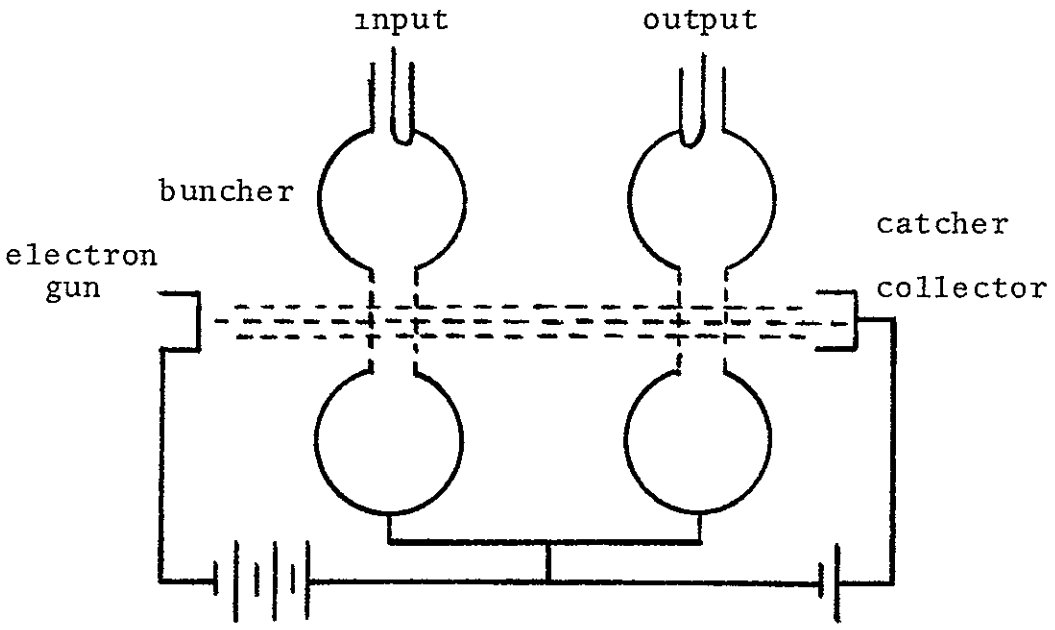

FIG. II-3 KLYSTRON SCHEMATIC

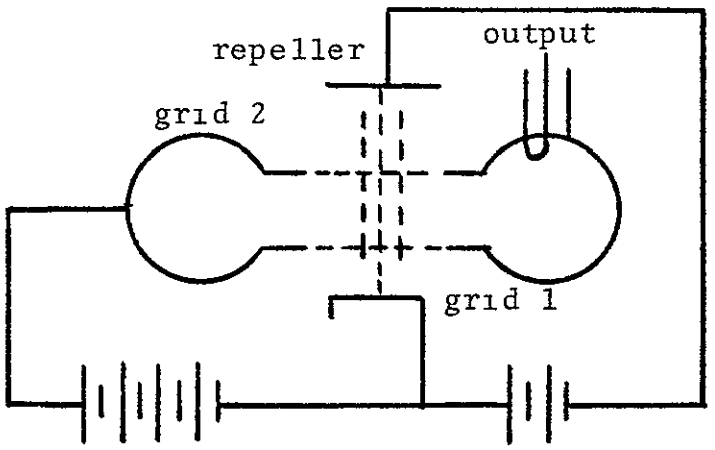

FIG. II-4 REFLEX KLYSTRON

tion in the other direction. The switches are designed such that the maximum switching rate is 45 KHz. When one switch is utilized to terminate flow of power from the klystron to the antennas, another switch allows passage of the signal reception to the receiving section and vice-versa Thus, the klystron is allowed continuous oscillation while the scatterometer operates as an ICW system.

The scatterometer output power can be transmitted either horizontally, vertically or time-shared between the two types to afford selective surface scattering modes This is accomplished using another ferrite switch which accomplishes the task of a ferrite circulator.

Two antennas are utilized to provide adequate isolation and dual polarization, one horizontally polarized and the other vertically polarized The antenna is a slotted waveguide in a duplexed scanning phased array. The beamwidth is about 120 degrees fore-aft and 3 degrees port-starboard Each hole on the slotted waveguide is associated with a ferrite phase shifter A beam steering computer is utilized to vary the current in the ferrite to change the phase such that the desired lobe position is obtained. The computer is designed to allow for 27 angles in the transverse direction for the lobe. The rate of transverse angular change is controlled by the

factor v/h, where h is the height of the aircraft and v is the velocity of the aircraft.

The ground area covered is dependent upon the time length spent viewing at each angle Certainly, total ground coverage is impossible using this scanning procedure, however, this is not the purpose of this design Instead, it is a general idea of ground roughness type, in the form of the backscatter coefficient, for comparison with coincident microwave radiometer data This matter will therefore have little significance in the equipment design. The ground coverage will be as shown in Fig. II-6.

Within this ground coverage, total radar backscatter will be placed on tape, however, the visual display will utilize only that portion of the data corresponding to the radiometer area coverage To do this, only data returning from a specified ground area must be filtered out of the total data return The method of filtering will be discussed later The ground area defining this specific area is referred to as the cell The cell is defined as having 75 foot length in the direction of flight (thus defining the doppler bandwidth) and a 3 degree areal coverage across Also specified for this defining cell is the aircraft height of 1,000 foot altitude and viewing angle of 50 degrees from the vertical in

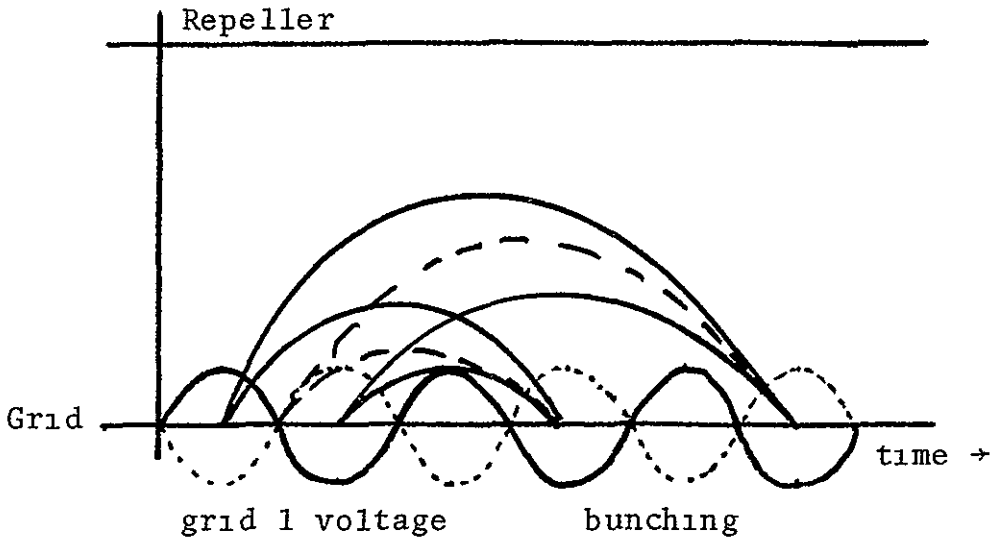

FIG II-5 REFLEX KLYSTRON VOLTAGE PATTERN

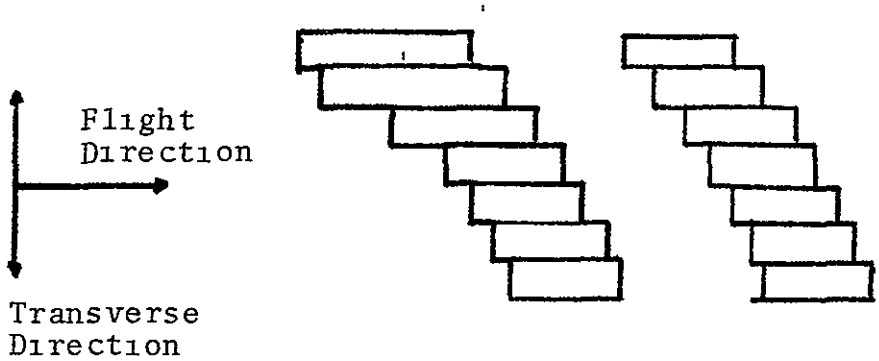

FIG II-6 SCATTEROMETER GROUND COVERAGE

the flight direction ($\phi = 0$). This determines the center frequency and doppler bandwidth of the area. As the fan beam angle moves off of $\phi = 0$, a variable low pass filter is adjusted such that the area viewed along a circular path 50 degrees from the vertical has the same ground length. The angle of scanning for the CRT data is always 50 degrees from the vertical, and will make a circular scan of the ground sweeping a ground arc of 72 degrees relative to the aircraft (Fig. II-7)

The cell definition was designed to make the scatterometer and radiometer viewing screens complementary. Even so, the basic cell can be adjusted if a more accurate determinance of backscatter coefficient is found to be necessary To do so, the fact that all ground coverage depends on the definition of the basic cell must be considered to see if system limitations are exceeded.

Reception

The returning signal is a function of the terrain scattering coefficient. It has a center frequency at the transmitted frequency 13.3 GHz but contains an envelope of the doppler frequency shift (f_d). In measuring the backscatter coefficient, f_d is utilized to specify ground position via frequency The envelope of the f_d spread is somewhat as shown in Fig II-8 The backscatter

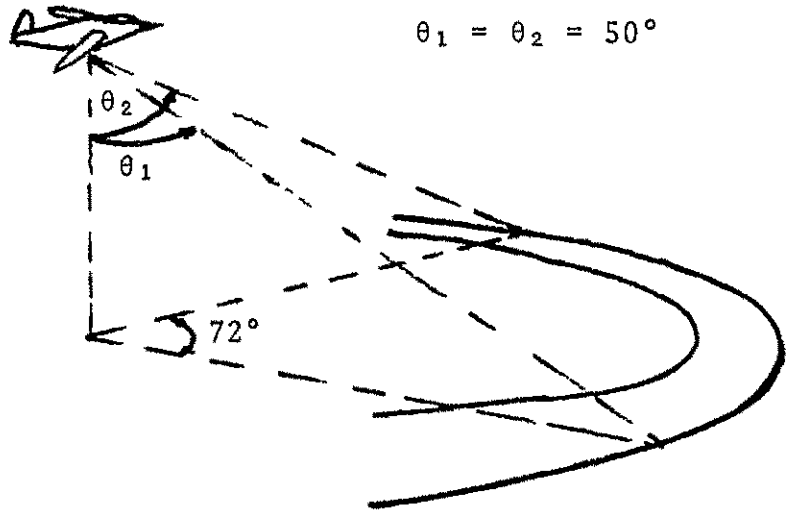

FIG. II-7 SCATTEROMETER VIEWING SCHEME

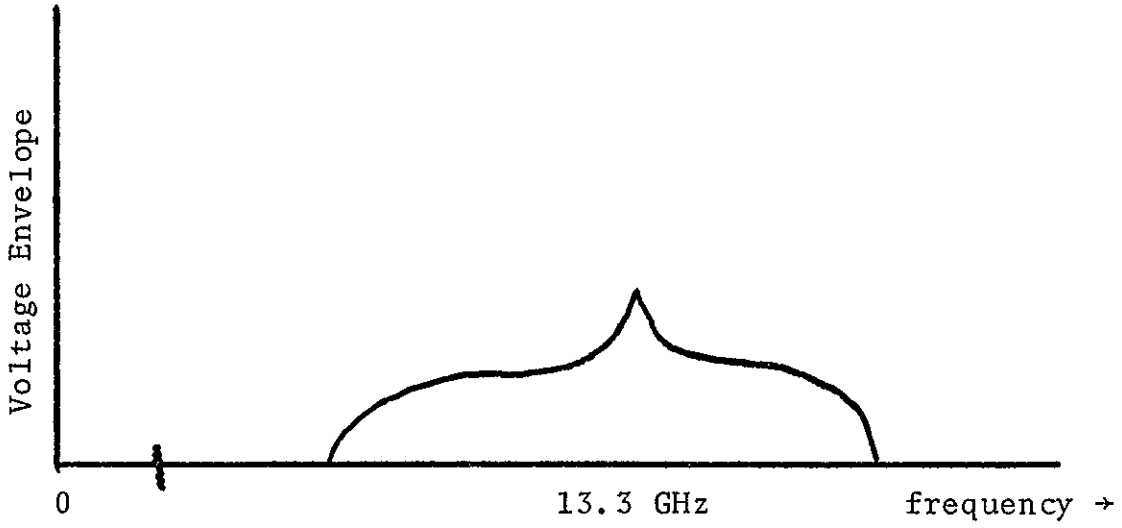

FIG. II-8 FREQUENCY SPECTRUM OF BACKSCATTERED SIGNAL

from vertical incidence is much greater than that from angles away from the vertical. When the fan-beam antenna lobe is pointed off vertical, the center frequency spike tends to deminish in size.

The frequency spread (approximately 21 KHz) will be constant in relation to the center frequency regardless of mixing. The spread in percentage of the center frequency, will change.

$$\% \text{ spread} = \frac{21 \text{ KHz}}{13.3 \text{ GHz}} = 1.6 \times 10^{-4}\%$$

$$\% \text{ spread} = \frac{21 \text{ KHz}}{250 \text{ KHz}} = 8.4\%$$

Increasing the percent of spread about the center frequency allows for less stringent design specifications for signal filters, such as the trap and low-pass filters

Another consideration concerning the return signal is that of conserving the return signal power Evaluation of the backscatter coefficient (σ_0) is directly dependent upon the magnitude of return power from a ground area. Since the determinance of σ_0 will have a variance, any uncorrected loss of power will have an adverse effect upon the variance. Therefore, steps must be taken to conserve power. Taking these two facts into consideration, the returning signal is subjected to frequency mixing to reduce the center frequency and is subjected to a calibration system to eliminate amplification

fluxuations. This affords easier signal handling and detects hardware effects upon power. The reception section of the scatterometer system is shown in Fig. II-9

The signal is received by the polarized antennas and passes through a circulator to the reception switch. When signal reception is desired, the signal proceeds through the mixer, where the center frequency is reduced, and to the logarithmic amplifier. The logarithmic amplifier is designed to equally amplify all portions, or frequency amplitudes. The trap filter is a band-eliminator filter which eliminates the high amplitude center frequency of the return signal. This eliminates the possibility that other circuit amplifiers will saturate. The problems with the mixer circuit are of great interest and will be discussed below.

The principle of frequency changing is basically simple. To accomplish the frequency change, the returning signal must be mixed with a signal at a frequency equal to the sum of the original center frequency plus the desired center frequency. The type mixer used and its construction is shown in Fig. II-10.

The mixing frequency is constructed such that the center frequency of the return signal will be added to the local oscillation of 250 KHz. To accomplish this, certain assumptions must be made. The klystron oscilla-

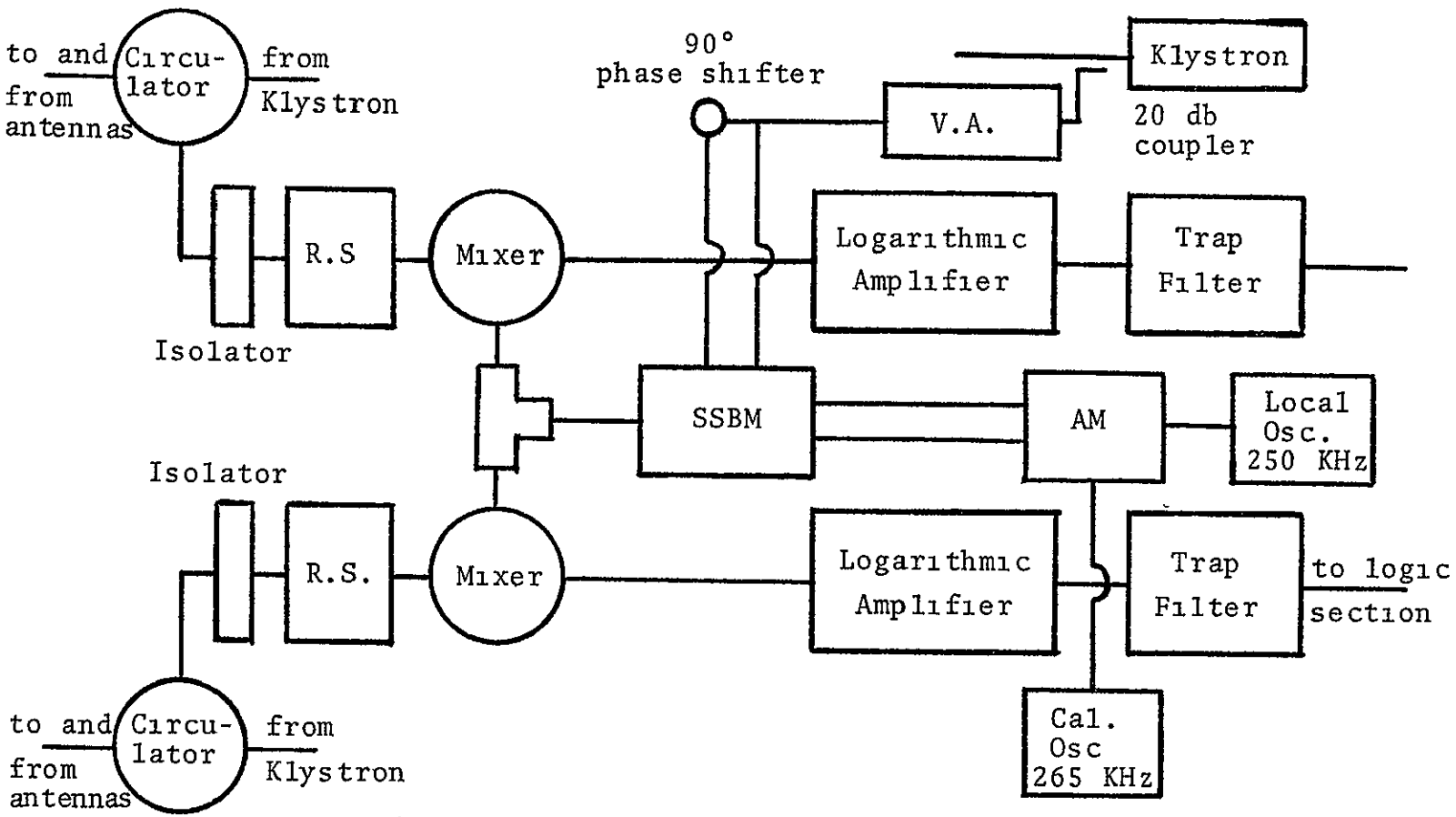

FIG II-9 SCATTEROMETER RECEPTION SECTION

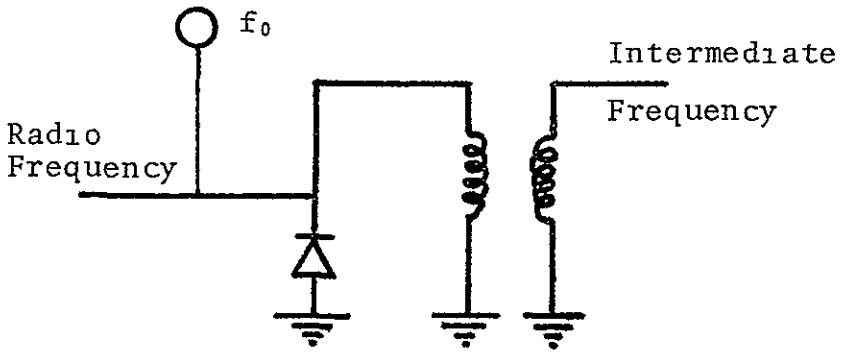

FIG II-10 SINGLE-ENDED MIXER

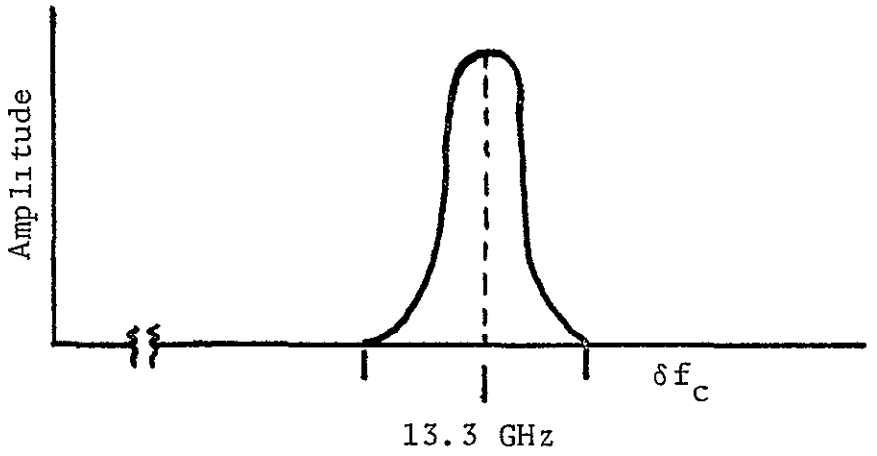

δf_c = variation about the center frequency

FIG. II-11 EFFECT OF FREQUENCY TRANSMISSION DRIFT

tion at 13 3 GHz is subject to drift over a small range due to cavity geometry This will appear as shown in Fig. II-11 This drift characteristic will vary with emitter and catcher voltage changes The power monitor provides constant amplitude, yet the drift is certain to occur If a drift in frequency has occurred since the transmission and mixer reception of the signal, the frequency spectrum after mixing has occurred will be

$$\left(f_c + \delta f_c + 250KHz\right) - f_c \pm \delta f_d$$

$$= 250KHz + \delta f_c \pm \delta f_d \qquad (2\text{-}7)$$

where δ = variation
f_c = center frequency
f_d = doppler frequency

Any δf_c will cause the signal reduction circuit, using doppler frequencies, to locate an area other than the desired area The possibilities of this happening can be avoided.

The maximum travel time, t_{max}, for the transmitted signal is

$$t_{max} = \frac{2h_{max}}{c\cos\theta} = \frac{2(10^4)}{\cos 50^\circ}\ \frac{1}{9.82\times 10^8}$$

$$= .32\times 10^{-4}\ seconds \qquad (2\text{-}8)$$

where C = speed of light
h = aircraft altitude

The doppler frequency change (Δf_d) in a cell block, say Δf_d = 287 Hz, is chosen to allow for an adequate number of independent samples to be received Therefore, for the cell to be completely missed in analyzation

$$\Delta f_d = \delta f_c = 287\ Hz \tag{2-9}$$

The frequency change per second occuring during the transmission time will be

$$\frac{\delta f_c}{t_{max}} = \frac{287}{.32 \times 10^{-4}} \cong 10\ MHz/sec \tag{2-10}$$

Klystrons having a frequency time drift of one-one-hundreth of this magnitude are available Therefore, proper selection of the ground area should not constitute a problem.

The local oscillation is introduced with the use of a single sideband modulator (SSBM) This SSBM receives the signals from the klystron and a local oscillator The local oscillation frequency of 250 KHz modulates the

13.3 GHz klystron signal creating signals of center frequency with upper and lower sidebands

The carrier frequency is denoted by

$$\chi(t) = A \cos \omega_k t \tag{2-11}$$

where $\chi(t)$= carrier signal
ω_k= is klystron frequency
A = is amplitude

The amplitude, A, of the signal after single sideband modulation is

$$A = A_c + k_1 A_m \cos \omega_m t \tag{2-12}$$

where. ω_m= is modulating frequency
A_c = is a constant value
k_1 = is a constant

The signal after single sideband modulation now becomes y(t)

$$y(t) = (A_c + k_1 A_m \cos \omega_m t) \cos \omega_k t$$

$$= A_c \cos \omega_k t + \frac{m A_c}{2} \cos(\omega_k + \omega_m) t$$

$$+ \frac{m A_c}{2} \cos(\omega_k - \omega_m) t \tag{2-13}$$

where $m = \frac{K_1 A_m}{A_c}$

The resultant frequency spectrum will appear as shown in Fig II-12

If there exists more than one modulating frequency, the spectrum will appear as shown in Fig II-13

Through all the reception hardware, the return power must be conserved and its amplication specifically known to eliminate any increase in σ_0 variance To accomplish this, a process of signal calibration is used to notice and correct for any system effect on power The system is designed to allow for a 4 0 db maximum loss in the system and for a 8.0 db maximum system noise level at 250 KHz If this is allowed to affect the variance, it will destroy the effectiveness of the system The effects of a slight power loss can destroy the system's ability to determine crop types, as can be seen from the crop db differences in Table II-2 [14].

Table II-2 data implies that a system having a two decibel variance in the σ_0 calculation can not determine between several crop types. The ability to construct the entire σ_0 vs θ curves is present, thus allowing identification by curve signature instead of only one angle. The problem of justifying the use of a single angle for identification depends upon eliminating the variance subjected to σ_0 by the system.

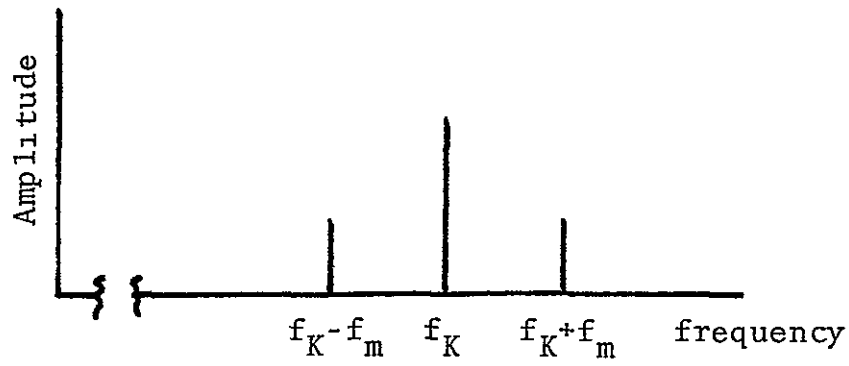

FIG. II-12 MODULATION FREQUENCY SPECTRUM

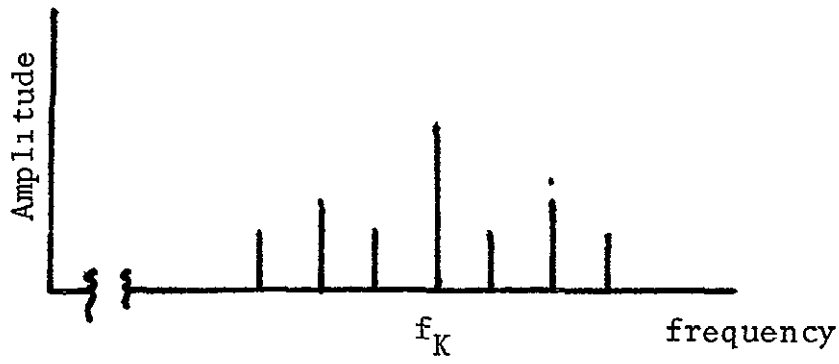

FIG II-13

MULTIPLE MODULATION FREQUENCY SPECTRUM

TABLE II-2

BACKSCATTER COEFFICIENT DATA AT A 50 DEGREE INCIDENCE ANGLE AND VARIOUS TRANSMISSION FREQUENCIES

Material	σ_0 Power Level In Negative db*	Frequency Used
Weeds on Dry Terrain	18 db	34 5 GHz
Weeds Over Wet Terrain	25 db	9 4 GHz
Wet Soybean Stubble 4 Feet Tall	10 db	35 GHz
Green Soybeans 3 Feet High	14 db	35 GHz
Oats 1/2 Inch High	16 db	35 GHz
Oats 4 Feet High	14 db	15 5 GHz
Wheat Stubble 12 Feet High	12 db	35 GHz
Green Wheat 1/2 Inch High	16 db	35 GHz

The transmitted power was used as the reference for the db scale

The method used to eliminate this variance is to inject another signal into the system and allow it to be subjected to all the return signals manipulations. The final calibration signal is then divided into the end results of the manipulated return signal to remove all gain and noise variations.

One proposed method of inserting this calibration signal is shown by the hardware schematic Here the calibrated signal combines with the local oscillator signal prior to entering the SSBM The SSBM amplitude modulates the klystron generated signal with the input signals.

The carrier and lower sidebands are eliminated and only the upper two sidebands emerge from the SSBM. This signal is injected into the mixer to produce a reduction in frequency of the returning signal. Both signals are equally processed. The final calculation of power for the 265 KHz signal is divided into the terrain signal power This corrects for gain and noise variations from the mixer to the divider.

Several problems are encountered by utilizing this method The major difficulty is that the returning power will adjust about 250 KHz. This can most easily be shown graphically (see Fig II-14).

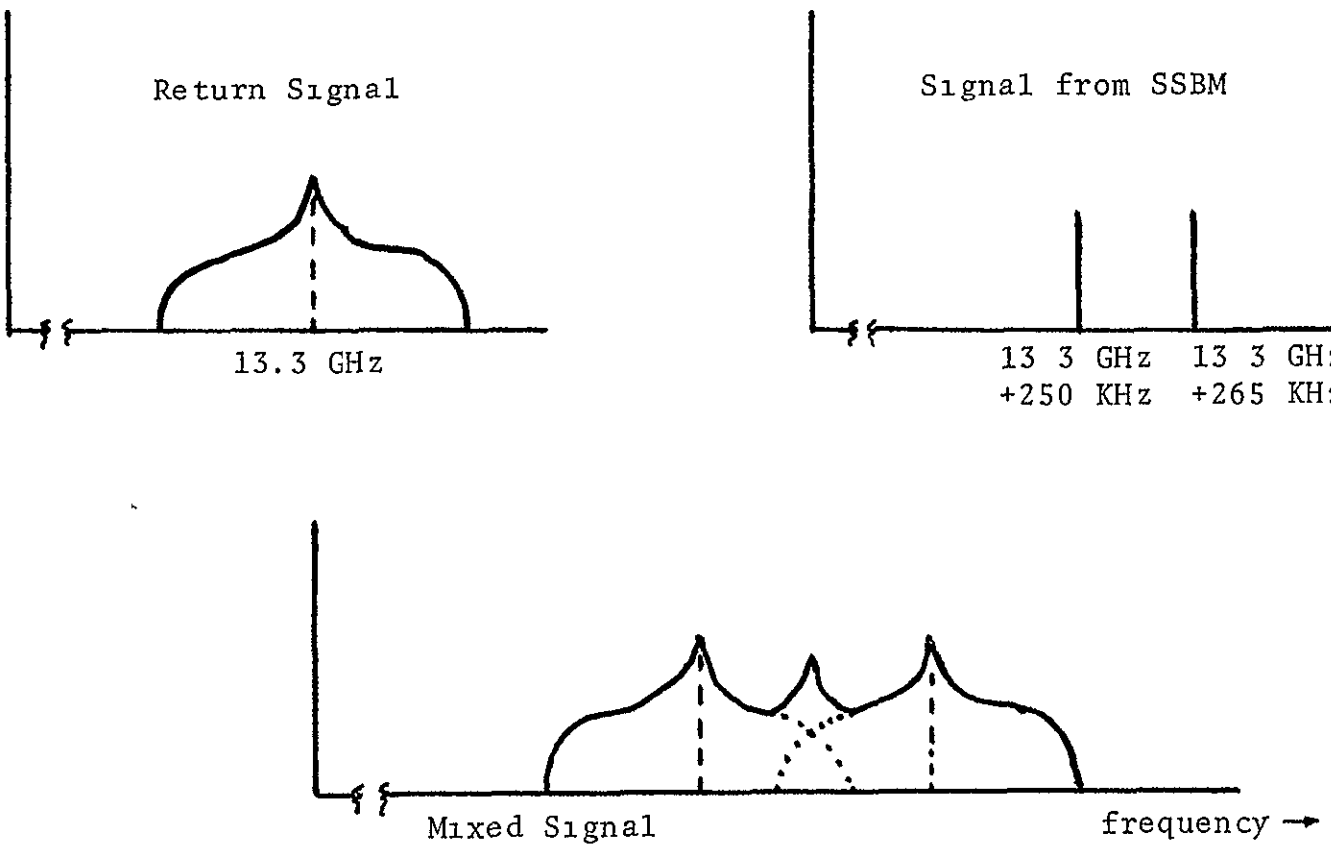

FIG II-14 POWER SPECTRUM OF MIXER OPERATION

The return power spectrum frequencies occur due to the forward viewing of the scatterometer This power is divided and inserted in the frequency spectrums about the two mixing frequencies. When the frequencies about 250 KHz are subsequently sampled, this power division will cause an incorrect σ_0 calculation to occur.

This method also eliminates utilization of those areas defined by the doppler shift of from 5-10 KHz. This occurs due to the doppler power impressed in frequency around 250 KHz and 265 KHz overlapping Backscatter coefficient calculations will therefore be incorrect for areas defined by these data points.

These effects nullify all advantages which might arise by utilizing this method of calibration. Thus another method of calibration needs to be implemented

Instead of the present method of continuous calibration being used, calibration for each hardware component could be implemented This would complicate the system due to the necessity of adding extra hardware.

Other methods of using continuous calibration are available The 265 KHz signal could be fed directly into the circuit after the mixer This would eliminate the type of power split previously mentioned and allow for continuous calibration of all components the previous method excluding the mixer.

Probably the best method would be that of using an altered SSBM to achieve the type of operation shown in Fig. II-15. Utilizing this method, the mixer output would be that of a spike at 265 KHz plus the doppler shift frequency around 250 KHz The power loss, amplifier flucuations, and system noise could then be accounted for and corrected The power split in the mixer would not occur

Signal Reduction and Logic

Once the signal has been received and the center frequency of the doppler frequency envelope has been reduced, the signal is processed to obtain the backscatter coefficient (σ_0) This processing or signal reduction section is shown in Fig. II-16.

Signal reduction is required to implement the real time CRT display. This signal reduction provides the σ_0 plus variance for each area viewed.

The signal, consisting of the doppler information and the calibration frequency, is passed through three amplifiers which allow for amplification of 30-70 db. The signal enters three circuits, one to allow for calibration, another to filter the desired doppler information, and the third to the flight recorder.

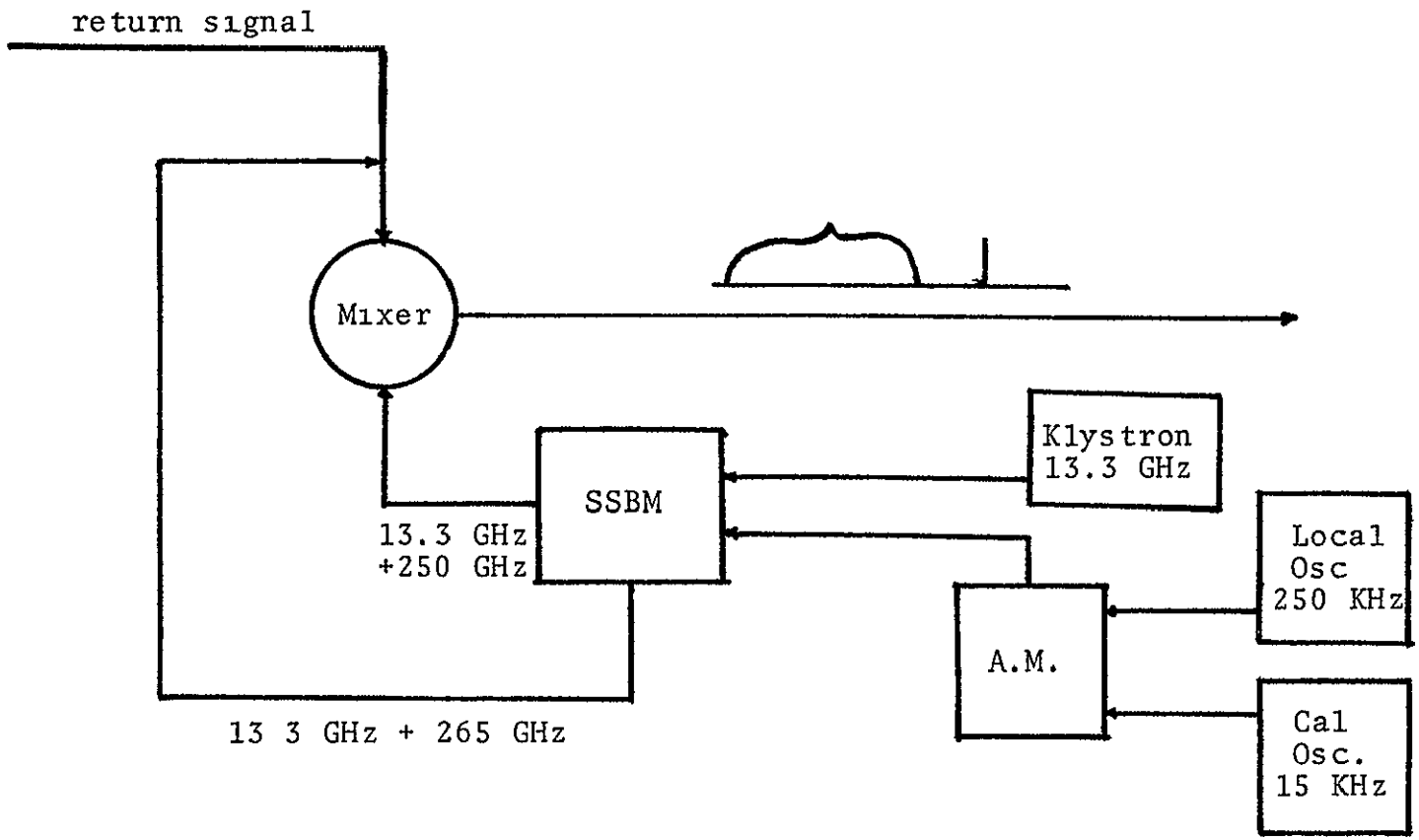

FIG. II-15 ALTERNATE RECEPTION SECTION

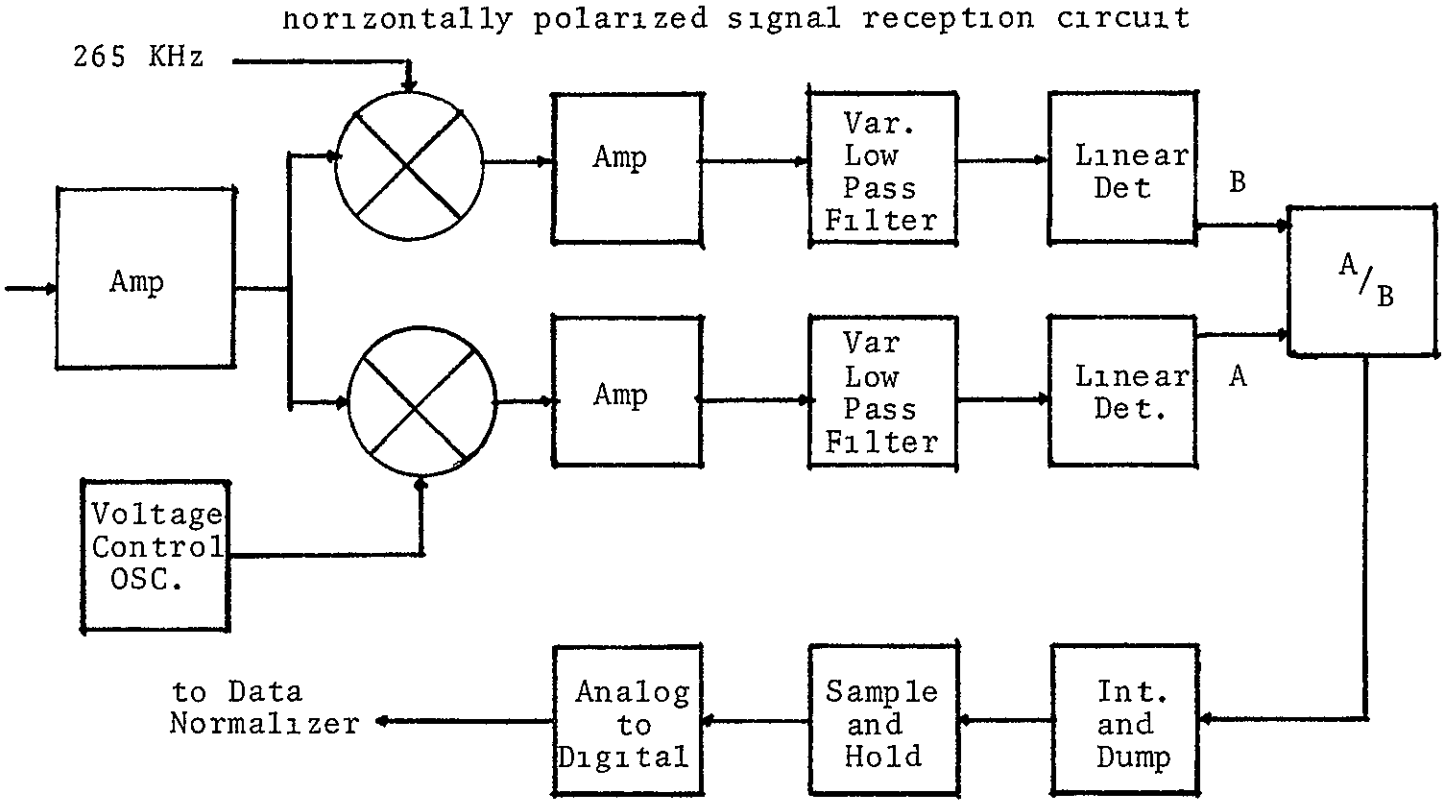

FIG. II-16 SIGNAL REDUCTION CIRCUIT

The signal to the flight recorder enters a mixer which transmits only the lower side band thus bringing the center doppler frequency of an area to zero hertz. This is accomplished by utilizing a voltage controlled oscillator (VCO) to generate the frequency desired for the mixer's local oscillation frequency

The use of doppler frequency for area delineation necessitates a frequency shift for the electronic processing A ground cell is defined by doppler frequency differences, for example 8064 Hz to 8300 Hz. This ground area would have a change in doppler frequency of Δf_d = 236 Hz (see Fig II-17) Only the area information defined by the Δf_d and the 3° beam width is desired. The VCO is biased to oscillate at the signal midpoint frequency of this area.

$$f_{VCO} = 250KHz + \frac{f_1 + f_2}{2}$$

$$= 250KHz + \frac{8064 + 8340}{2}$$

$$= 250KHz + 8182Hz \qquad (2\text{-}14)$$

where f_1, f_2 = lines of constant doppler frequency shift which delineate a ground cell

This frequency, f_{VCO}, for this area is fed into the mixer The mixer creates a signal of frequency spectrum

resembling the diagram in Fig II-18 Part of the previous frequency spectrum (i.e 250 KHz) is folded over onto itself causing the voltage amplitude in this region to add.

The signal is amplified and passes through a variable low pass filter (VLPF) The amplifier is designed such that the information previously at 8182 Hz, now D-C, will be amplified, thus retaining information at this point This restriction can be eliminated if the information lost is quite small compared to the total information reflected from the area under consideration The D-C amplification is necessary due to the nature of the calibration techniques used. Another restriction is that the amplification must be almost constant over the frequency range from 0-1000 Hz for reasons to be shown later

The frequency response of the VLPF is controlled from the synchronizer The frequency response varies to compensate for velocity and scan angle variations This VLPF variation is necessitated by the geometry of the CRT display If the frequency response of the VLPF was held constant, the ground area represented by the filtered frequency range Δf_d would vary This occurs due to the nonuniformity of the lines of constant doppler frequency (see Fig. II-19).

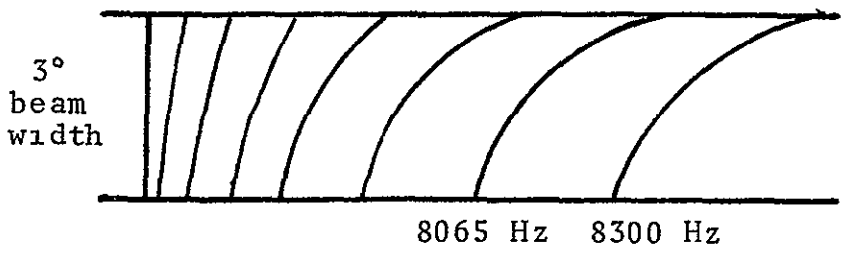

FIG. II-17

GROUND APPEARANCE OF LINES OF

CONSTANT DOPPLER FREQUENCY

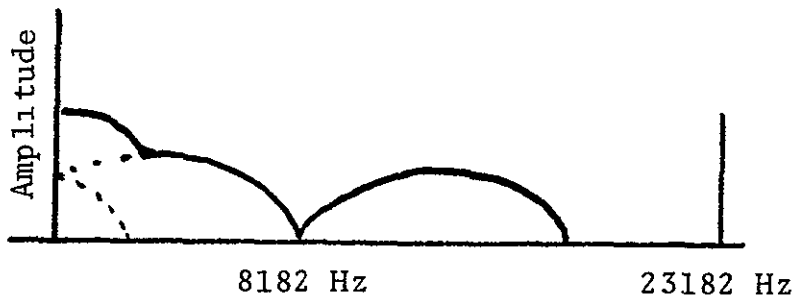

FIG. II-18

MIXER SIGNAL OUTPUT

To keep the area constant for each cell at any angle, the frequency response (f_r) of the filter (i e. equal to $\frac{1}{2}\Delta f_d$ in Hz) must vary. To analyze only the frequency spectrum of the hypothetical area, the VLPF frequency response will be

$$f_r = \frac{1}{2}\Delta f_d = \frac{1}{2}(236\,Hz) = 118\,Hz \qquad (2\text{-}15)$$

The response in only one-half of the doppler frequency representing the area since the frequency spectrum in f_r is the folded-over spectrum area from the mixer The information contained in f_r is equal to that contained in Δf_d. The frequency response f_r is not likely to exceed 1000 Hz. Therefore, the amplification level of the amplifier in this circuit needs only to be flat in the frequency range 0-1000 Hz.

The signal now enters a linear detector. This reduces the signal to the voltage envelope as shown in Fig. II-20

The reason for considering voltage here instead of power is explained through the operation of the calibration system As mentioned previously, the signal from the three amplifier stages enters three circuits, one of which is the calibration signal reduction section Since

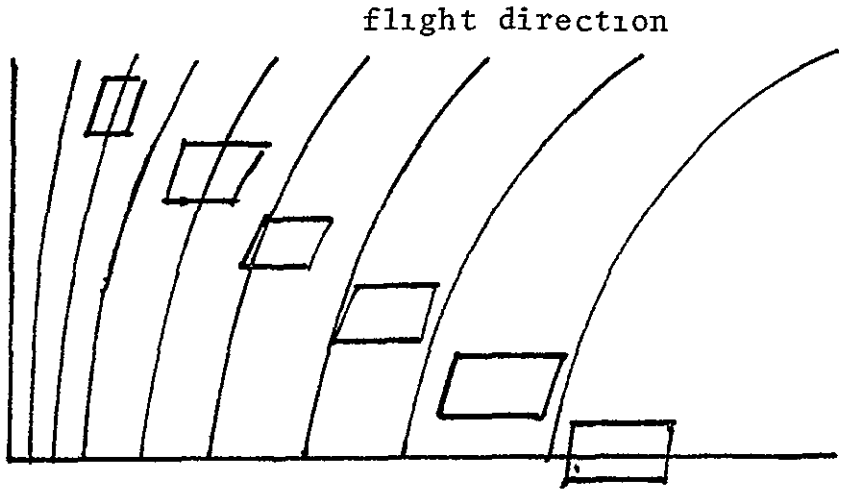

FIG. II-19

SCATTEROMETER GROUND VIEWING

FOR CONSTANT DOPPLER FREQUENCY

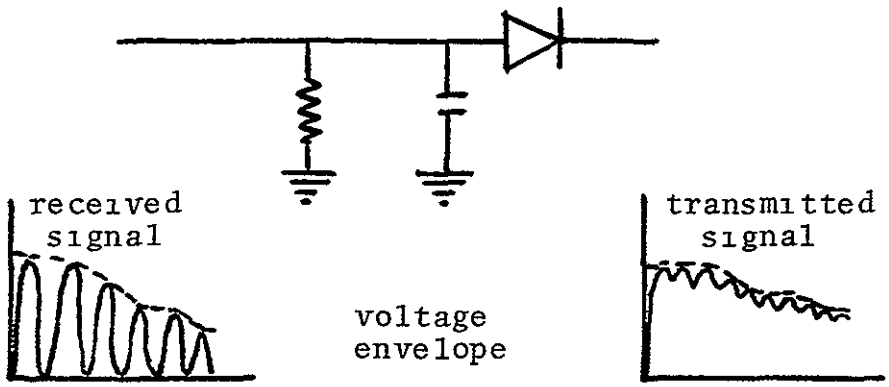

FIG II-20

A LINEAR DETECTOR

the three circuits are in parallel, the voltage levels at all frequencies entering these circuits will be equivalent. Up to this point power conservation has been a main goal. The voltage relationships now have to be considered such that equivalent signals will pass through both the calibration signal and doppler signal reduction sections Loss of power, however, must be avoided. Power is now considered in one of its representative forms.

$$P = VI = V\frac{V}{R} = \frac{V^2}{R} \qquad (2\text{-}16)$$

where P = power
V = voltage
R = resistance
I = current

If the impedance of the reduction circuits for the calibration signal and doppler signals are equivalent, a power ratio would be equivalent to

$$\frac{P_d}{P_c} = \left(\frac{V_d}{V_c}\right)^2 \qquad (2\text{-}17)$$

where d = implies doppler
C = implies calibration

This power ratio will occur later in the final operation of the calibration system. Therefore further operations will be concerned with voltage levels.

The amplified return signal initially enters a mixer in the calibration signal reduction section. The calibration oscillation signal (265 KHz) is mixed with this signal. The mixer transmits only the lower side band The calibration signal in the return signal is therefore beat to zero hertz. The resultant spectrum is shown in Fig. II-21

The signal enters an amplifier equivalent to that in the doppler signal reduction circuit This amplifier must amplify D-C in order for the calibration signal to be subjected to the same treatment the doppler signal receives in its reduction circuit.

The amplified signal passes through a variable low-pass filter comparable to that contained in the doppler signal reduction circuit The frequency response f_r of this VLPF is equal to the f_r in the other reduction circuit. This causes the impedance values of both VLPF's to be equivalent.

The D-C calibration signal is now transmitted to a linear detector which also is comparable to the one con-

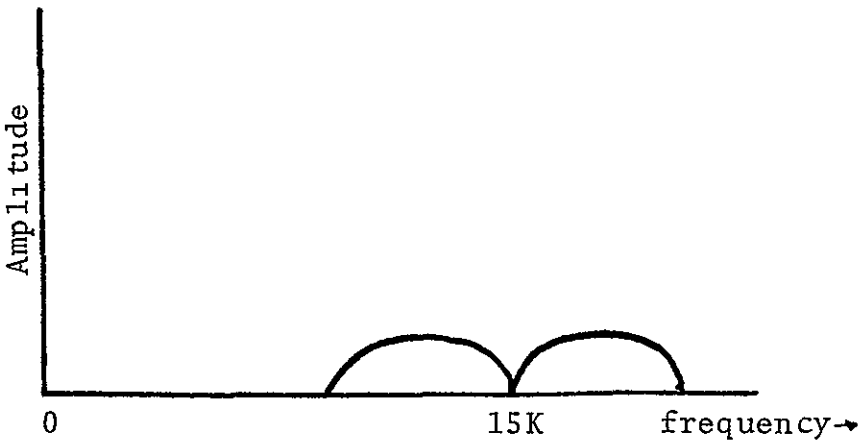

FIG II-21

RESULTANT SPECTRUM AFTER MIXER

OPERATIONS IN CALIBRATION REDUCTION CIRCUIT

tained in the other reduction circuit. The return signal is therefore subjected to equivalent operation, except for the beat frequencies in the mixers, in both reduction circuits This means that the resistive effects of both circuits are equivalent and that the use of voltage vs. power handling is justified upon the division of the two resultant signals.

The signals from the two reduction circuits enter an analog divider. Using voltage magnitudes, the signals will be passed through diodes whose output response will be the logarithmic value of the input. The two logarithmic signals are then subtracted. This value is doubled to account for the voltage squaring in order to represent the power ratio The signal is then passed through an antilog device to obtain the final signal output

There exists the possibility of using power magnitudes for operations in the analog divider. Since the impedance values in both reduction circuits are equivalent, the signal power entering each of these circuits will be equal The power entering each of these two circuits will be less than one-half of the previous total power due to power also entering the third parallel circuit. After the signals are processed, the power contained in the calibration signal ($a \cdot P_C$) is an equal fraction of its previous value as is the power contained in

the doppler frequency signal ($a \cdot P_d$) The analog divider must be designed such that the logarithmic values of the power magnitudes is obtained, subtracted, and the anti-logarithmic power magnitude acquired

$$\ln aP = \ln a + \ln P$$

therefore

$$\ln aP_d - \ln aP_c = \ln P_d - \ln P_c = \ln \frac{P_d}{P_c} \qquad (2\text{-}18)$$

where a = constant

Whichever signal process is chosen, the calibration signal must be designed such that its logarithmic value represents signal variance in the system This requires that the signal magnitude of the reduced unaffected signal will give a logarithmic value of zero This would indicated that the return signal was also unaffected by signal noise and losses If this final reduced calibration signal is different from the specified value, its logarithmic value will not be zero Then, the division process will correct the doppler signal to its unaffected value, assuming the doppler signal and calibration signal were equally affected by the system

After all gain variation has been removed by the analog divider, the signal enters the integrate-and-dump section. This section acts much like a charging capacitor in which many return signals are allowed to add. The signal will appear as shown in Fig. II-22. When a certain time limit is reached, the voltage value obtained is discharged and passed into the sample-and-hold section.

The integration technique used here must actually find the average value of all the input signal voltages. The pulse rate frequency 45 KHz, or 225 KHz, determines the number of input signals.

If the reception occurs for .2 seconds during the 45 KHz PRF, nine thousand signal voltages will be placed into the integrator The voltage value sent to the sample-and-hold section must be the average of all of these signal voltages. This is quite easily attained. An example of how this can occur is shown in Fig II-23 The signal voltages will charge C_1. During the period of antenna lobe reajustment, no signal is coming into the integrator, thus, the voltage across capacitor C_1 will be accumulation of the 9000 signal voltages Then switch S_1 is thrown. The capacitor C_1 will discharge its voltage as

$$V_{C_1}(t) = V_{max}\, e^{-\frac{1}{R_1 C}t} \qquad (2\text{-}19)$$

where $C = C_1 + C_2$

The voltage will be allowed to discharge until $\exp(-\frac{t}{R_1 C}) = \frac{1}{9000}$ then, the voltage across capacitor C_2 will be one nine-thousandth of the maximum voltage and thus, the average voltage When this time occurs, switches S_1 and S_3 are thrown. Capacitor C_1 retains its average voltage value and capacitor C_2 discharges rapidly The process of capacitor C_1 recharging starts again. Prior to S_1 being thrown again S_2 is closed, then opened, to discharge capacitor C_1 and thus prepare it for its next charge

This is just one method of integrating-and-dumping plus sampling-and-holding Switches S_1 and S_2 must be thrown in their proper sequence during the antenna lobe readjustment period This period is quite small and thus sets quite stringent specifications for this part of the system and its operations. Whatever method is used, it will follow these lines It must be noted that this is just one of the many possible methods of integrating and sampling

The analog-to-digital converter has a switch in series with an extremely large resistance. The switch

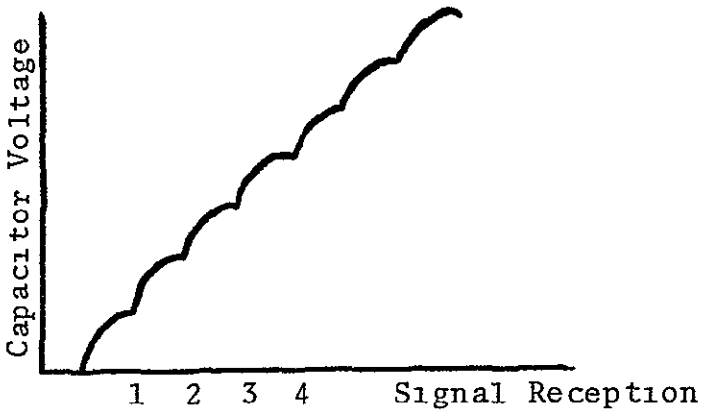

FIG. II-22

VOLTAGE REPRESENTATION OF SIGNAL INTEGRATION

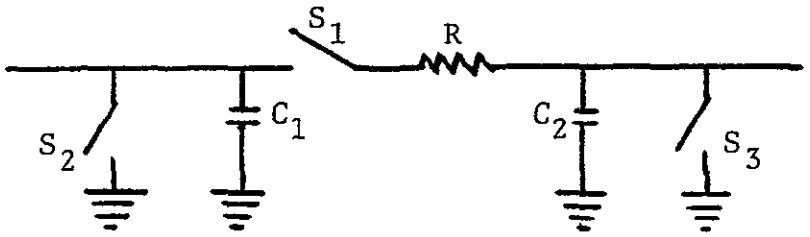

FIG. II-23

EXAMPLE OF INTEGRATE AND DUMP CIRCUIT

will be thrown, thus sampling the voltage, without too much voltage drain. The signal is then in digital form for normalization purposes

Using this average return power, the backscatter coefficient can be determined by utilizing the radar equation, [18]

$$W_s = \frac{P_t G_o^2 \lambda^3 \bar{\sigma}_o f_1(\theta) f_2(\theta,\phi)}{2(4\pi)^3 h^2 v} \qquad (2\text{-}20)$$

where
W_s = averaged return power
G_o = antenna gain
λ = transmitted wavelength
$f(\ )$ = antenna pattern functions
θ = incidence viewing angle
ϕ = transverse viewing angle
h = aircraft height
v = aircraft velocity
$\bar{\sigma}_o$ = average backscatter coefficient

This equation is rearranged to obtain an equation for the backscatter coefficient

$$\bar{\sigma}_o = \frac{W_s 2(4\pi)^3 h^2 v}{P_t G_o^2 \lambda^3 f_1(\theta) f_2(\theta,\phi)} \qquad (2\text{-}21)$$

This operation occurs in the data normalizer section. A block diagram representing this section and its inputs is shown in Fig. II-24.

The received signal will appear as shown (Fig II-25) during the passage through the signal reduction section

The final pieces of hardware in this section of the scatterometer are the synchronizer and its accompanying equipment This hardware constitutes the logic section and governs all scatterometer operations. A block diagram of this hardware appears as shown in Fig. II-26.

The synchronizer commands will determine the variance of the determined σ_0 from its true value As shown previously, this variance is determined by the number of independent samples (N_1) This N_i is

$$N_1 = \frac{\text{time to pass a resolution element of width } \Delta\rho}{\text{time per independent sample}}$$

where: time/sample = $\frac{1}{4\Delta f_d}$

therefore

$$N_i = \frac{\Delta\rho/V}{1/4\Delta f_d} = \frac{4\Delta f_d \Delta\rho}{V} \qquad (2\text{-}22)$$

where V = velocity of the aircraft

The velocity and antenna patterns control the effectiveness of the system. Also, the increase of the reception

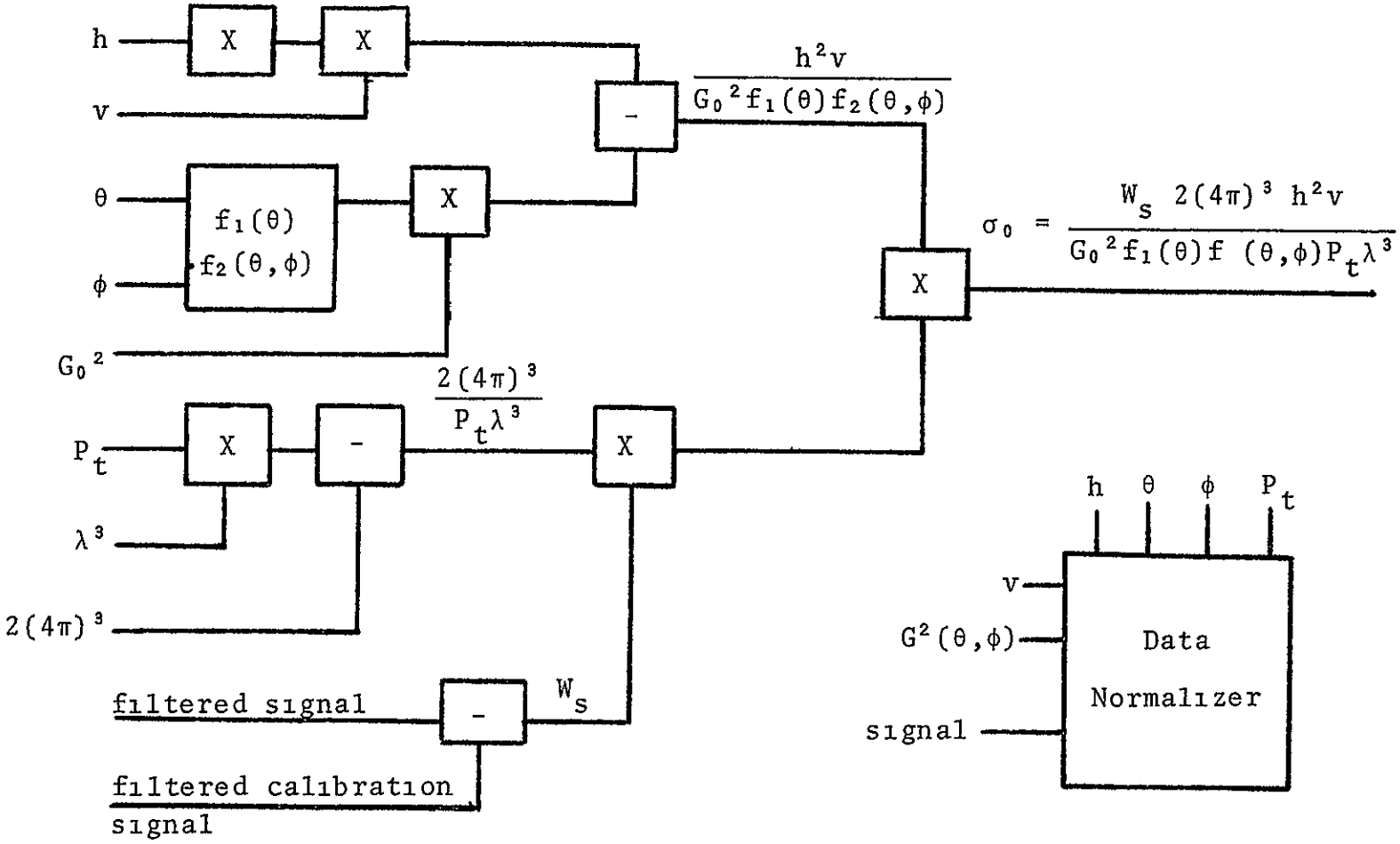

FIG. II-24 THE DATA NORMALIZER

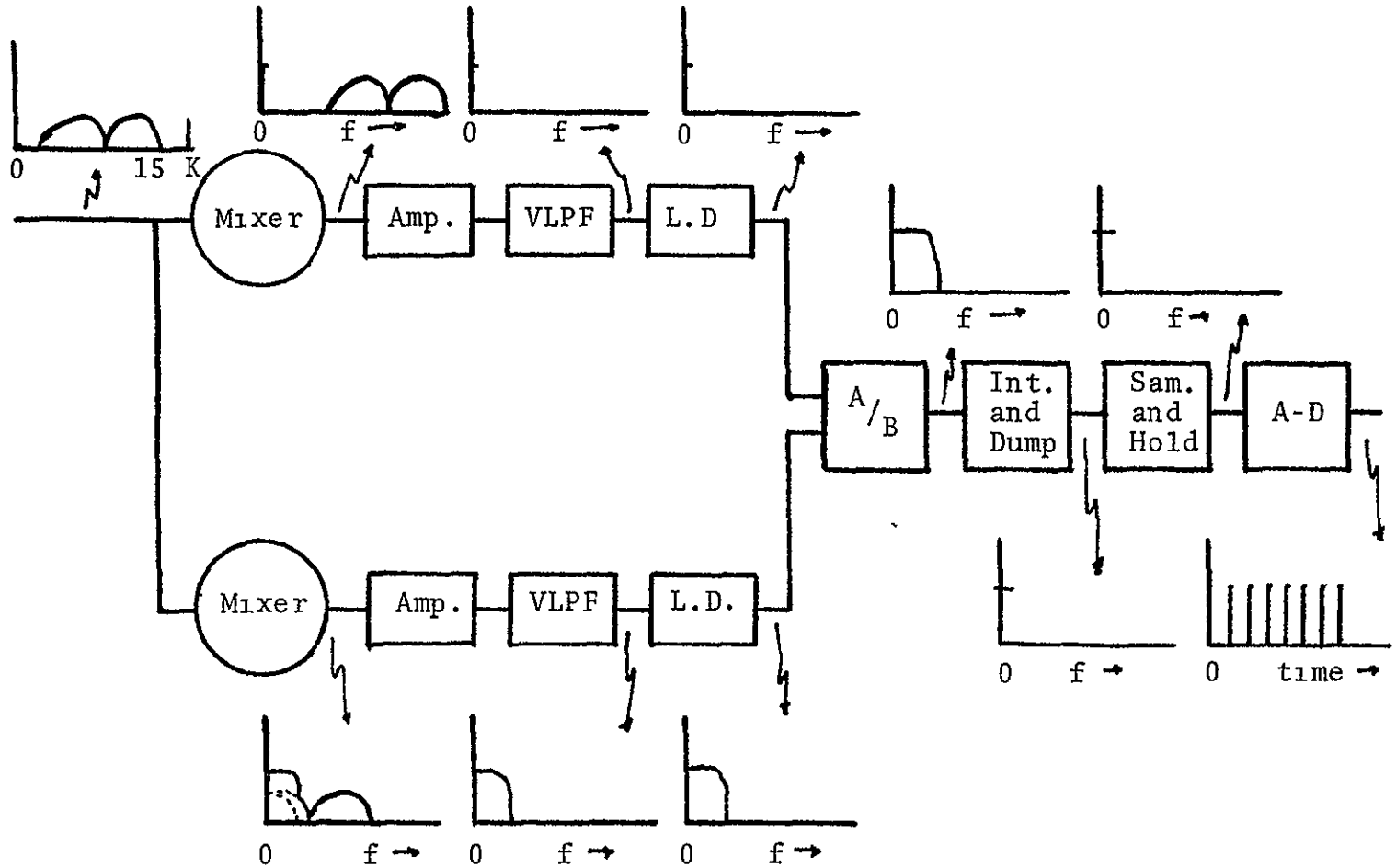

FIG. II-25 SIGNAL VOLTAGE ENVELOPE SPECTRUM AFTER VARIOUS OPERATIONS

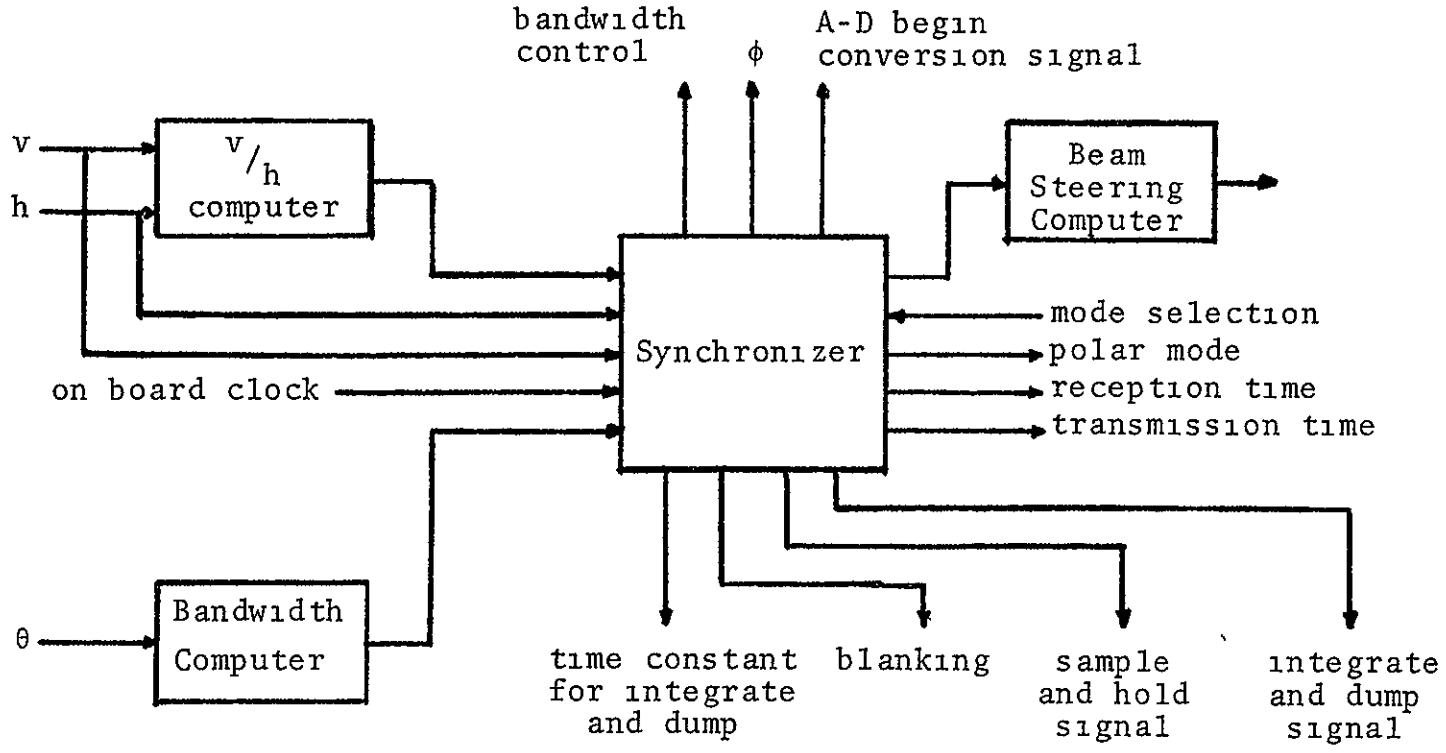

FIG. II-26 SYNCHRONIZER INPUT AND OUTPUT

and integration times will increase N_1. This will also affect the effectiveness of the system. Thus, the design and operations of the synchronizer play a dominant role in the usefulness of the scatterometer

Recorder

The returning signal contains information from ground areas at all angles of incidence up to and including 50°. It is desirable that all of this information be retained. A tape recorder system shown in Fig II-27 is utilized to record on dual track tape information in analog form for subsequent processing One track is open for the signal from the horizontal reception circuit and the other for the vertical reception circuit.

The signal is received from the reception portion and passed through the three amplifiers. A code oscillation is injected into the third amplifier of the circuit that is receiving the cross polarization component The recorder is receiving either the return signal or the code oscillation. Thus, when the code signal is transmitted through the vertical reception circuit, the horizontally polarized return is being recorded When the code signal is transmitted through the horizontal reception circuit, the vertically polarized return is being recorded. This is useful during post-flight evaluation

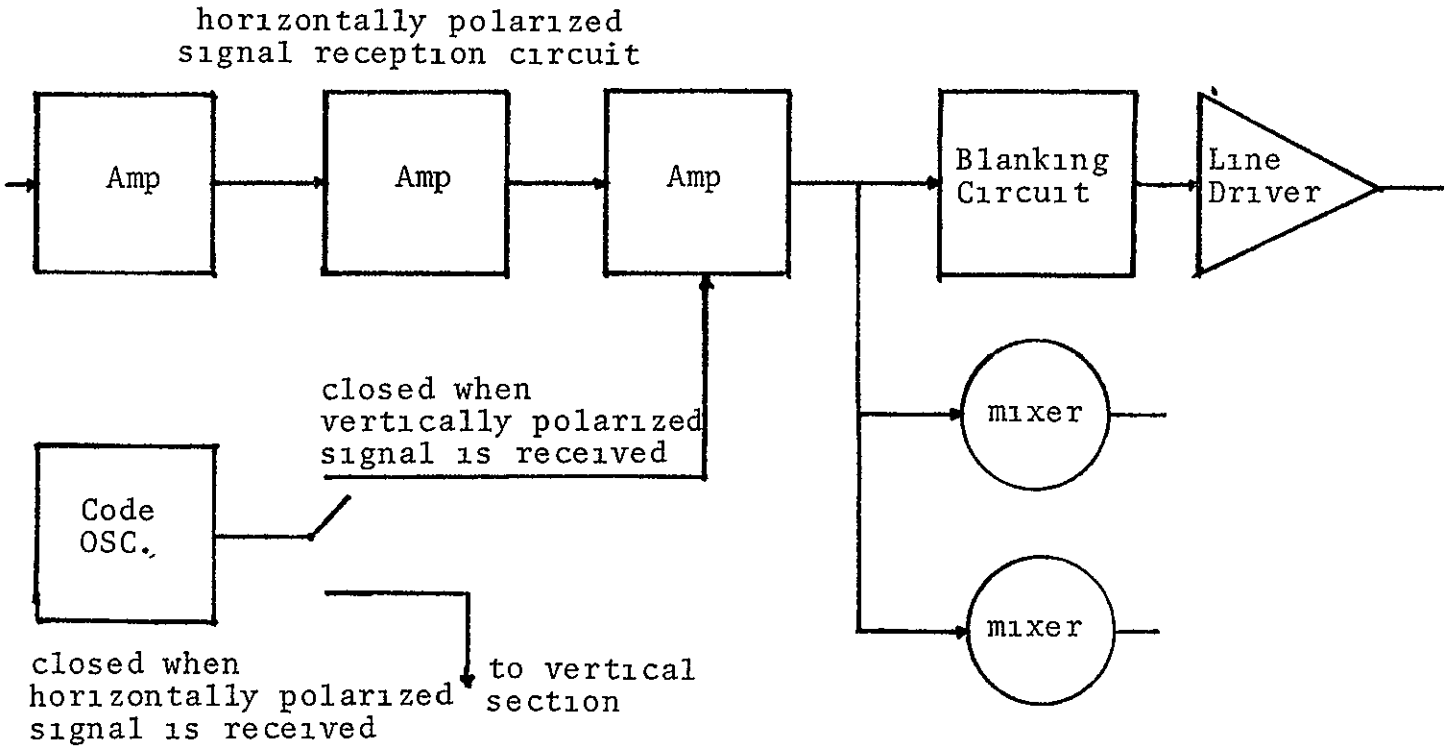

FIG. II-27 RECORDER CIRCUIT

for piecing together the horizontal and vertical tape portions.

The blanking circuits are used to eliminate passage of any signal during the period of antenna lobe adjustments. This eliminates any spurious signal from the antenna, code oscillator, or system from being recorded as a signal during this period

The line drivers are used for impedance matching purposes They are designed to operate over the frequency range of 150 KHz to 350 KHz with less than 1% amplitude and frequency distortion.

This taped signal will be used for post-flight evaluation of σ_0 vs. θ for those areas which this is possible This signal is in analog form on the dual tape track for purposes of distinguishing between horizontally and vertically polarized reception Post-flight evaluation will utilize the identical signal reduction and logic section of the scatterometer The required adjustments will be made to allow for σ_0 vs. θ evaluation for θ other than 50°. The procedure for accomplishing this will follow from the information given about the signal reduction circuit.

CRT Display

After signal normalization occurs, a value of σ_0 is obtained and transmitted to the cathode-ray-tube display circuit (Fig II-28)

The display circuit receives the signal as a voltage representation of σ_0 The information from all the areas on a single sweep appear on the display as the top line after having been released by the scan storage and passed through the digital-to-analog converter. The analog signal is necessary for continual CRT sweep This information was also transmitted back into the gate which will then release information from the newest sweep and subsequently this returned information. The analog information is used to intensity modulate the signal of the CRT display As the information is transmitted to the gate and released prior to newer information, the display shows the σ_0 information declining, hence the falling raster technique. This will appear as shown in Fig. II-29.

Since a great deal of effort is expended in evaluating σ_0 as correctly as possible, the screen brightness should adequately represent the signal voltage value. A curve of input voltage vs. output brightness in lumens will appear as shown in Fig. II-30

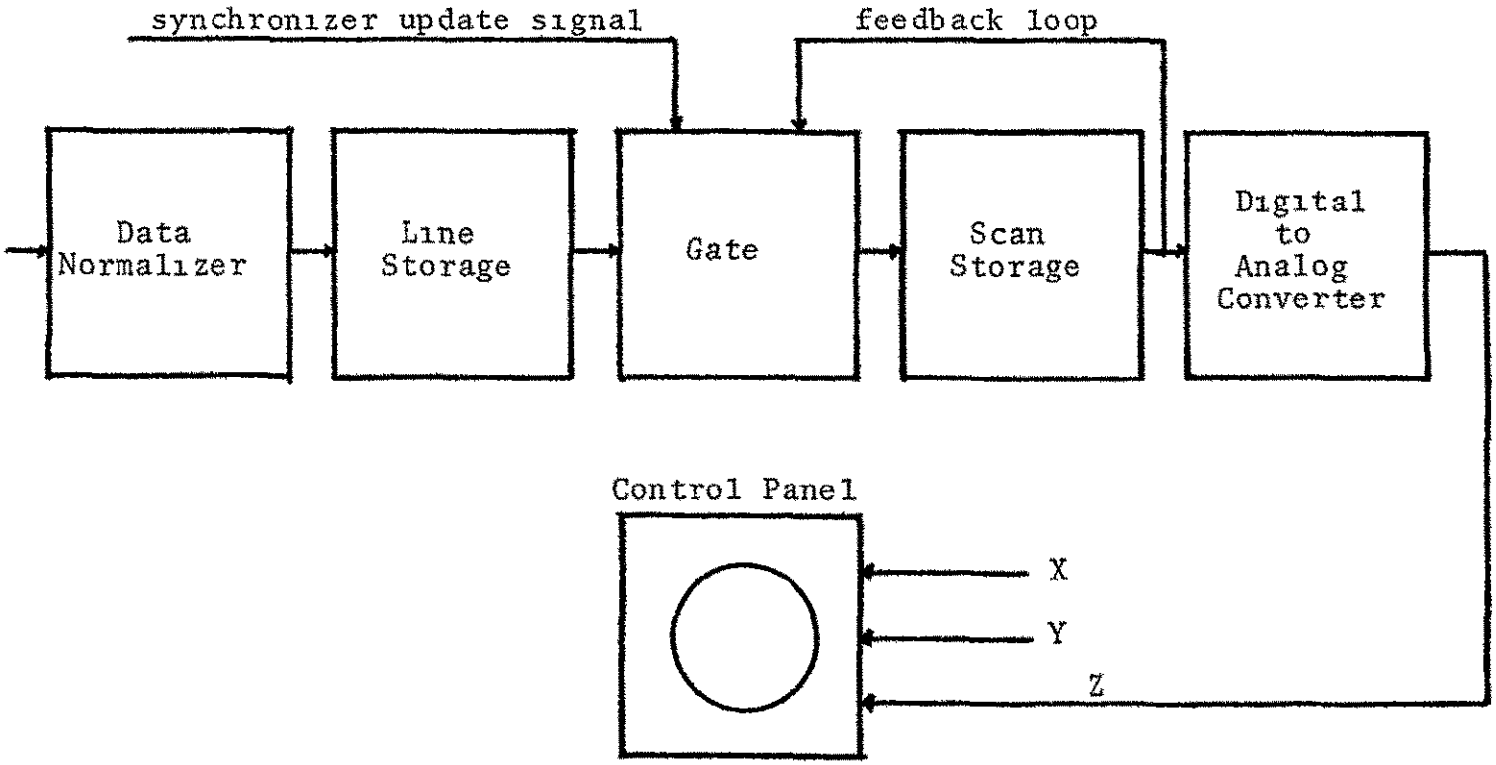

FIG II-28 CRT DISPLAY CIRCUIT

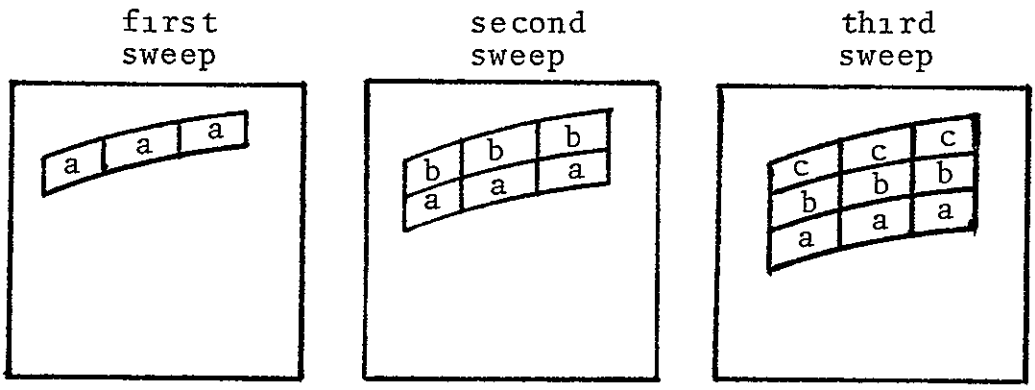

FIG II-29

FALLING RASTER TECHNIQUE

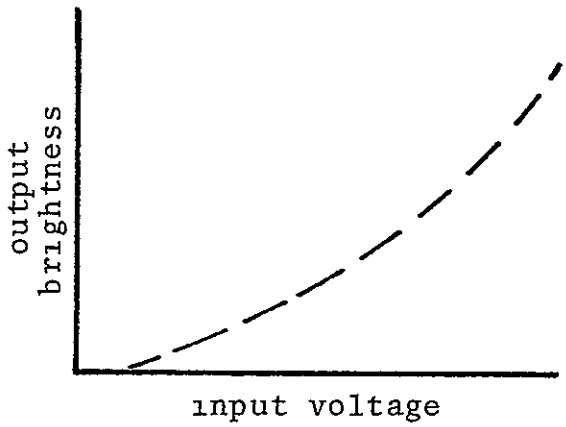

FIG. II-30

BRIGHTNESS VS VOLTAGE

CURVE FOR CRT DISPLAY

This curve in non-linear. Therefore a gamma-correction factor is required in the display circuitry to adjust the input voltage. This causes the curve to in effect become linear, thus adequately representing σ_0 through brightness [19].

CHAPTER III

MEAN DETERMINANCE OF A BACKSCATTER SIGNAL USING A HALF-WAVE LINEAR DETECTOR

Signal backscatter is subject to fading. The signal reflected from the ground and received at a point above the ground will have amplitude variations commensurate with slight variations of the receiving point This occurs because the signal received is the vector sum of all the individual returning signals existing at that point Thus, at a different point, the vectors will be different and will produce a different sum. Therefore, for an aircraft flying over the reflecting ground, the return signal will be subject to fading.

The scatterometer described in Chapter II integrates the return signal, from a ground cell having a doppler frequency difference of 280 Hz viewed at an angle of 50°, for periods of 0 2 seconds The scatterometer will integrate and average numerous transmitted, and subsequently reflected, pulses. If the pulses reflected from a specific ground area were averaged over an infinite length of time, a true mean or average signal value could be found. Since infinite time averaging is impossible, it becomes necessary to find how the finite time average approximates the true mean signal value reflected from

the ground This involves determining the variance or decibel range about the true mean signal value within which the finite time average is located. These values will be found for the operations of the scatterometer described in Chapter II. Also, possible improvements for the scatterometer averaging are given.

Fading

If the transmitted signal wavelength is large in comparison to the ground distance required for appreciable slope change, the ground is considered "smooth". The signal reflection from the smooth surface will follow Snell's Law of reflection. Snell's Law depicted in Fig. III-1, states that a ray incident upon a surface makes an angle with the surface normal which is identical with the angle the reflected ray makes with the surface normal. This law is the basis of all geometrical optics observations It applies only for smooth surfaces. The determination of a surface being smooth depends upon the individuals definition of large and appreciable in reference respectively to wavelength and slope change.

Similarly, if the signal wavelength is small in comparison to ground variations, the ground is considered "rough" Statistical distribution methods are used to

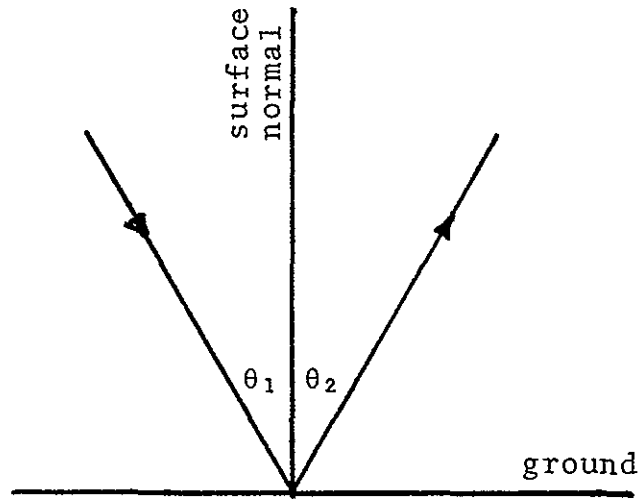

angle of incidence, θ_1, equals angle of reflection, θ_2, for a smooth surface

FIG. III-1 SNELL'S LAW OF REFLECTION

determine the signal reflection or scattering from a rough surface. These methods will define the surface roughness and will determine the distribution of the amplitude and phase of the scattered field. Nearly all natural terrain surfaces can be assumed "rough".

Statistical methods, which define a rough surface, describe the distribution of the surface height deviations from the mean or average level with a density curve. One type of density curve, the Gaussian, often arises as the solution to scattering from rough surfaces The Gaussian density function is described for a one dimensional surface as

$$f(x) = \frac{1}{\sqrt{2\pi\sigma^2}} e^{-\frac{(x-\eta)^2}{2\sigma^2}} \qquad (3\text{-}1)$$

where η = the mean or average height
$f(x)$ = the density function
σ^2 = the variance about the mean

As the variance, σ^2, approaches zero, the Gaussian distribution will bunch about the mean value until, when $\sigma^2 = 0$, the density function will be a unit impulse located at the mean value.

Another density function which is used to describe

surface and signal amplitude distributions is the Rayleigh density function, given by [20]

$$f(x) = \frac{x}{\alpha^2} e^{-\frac{x^2}{2\alpha^2}} U(x) \qquad (3\text{-}2)$$

Some properties of these curves are that they are non-negative and that the area under the curve is always equal to one.

$$\int_{-\infty}^{\infty} f(x)\,dx = 1$$

The mean value η can be found from the density curves using the expected value technique, where $E\{\ \}$ is the expected value

$$\eta_x = E\{x\} = \int_{-\infty}^{\infty} x\, f_x(x)\, dx$$

$$E\{x^n\} = \int_{-\infty}^{\infty} x^n f_x(x)\, dx$$

The variance, or amount of deviation around the mean value, is used to define the range of values that the distribution assumes. It is defined as σ^2.

$$\sigma_x^2 = E\{(x-\eta_x)^2\} = E\{x^2\} - E^2\{x\}$$

Signal fading necessitates time averaging the signal in order to evaluate the mean value of power reflected from a surface type. This mean value is utilized to provide an estimation of the overall roughness of the ground area viewed. Knowing the variance that the averaged power value has from the mean value, the approximate backscatter coefficient can be calculated [21].

$$\sigma_o = \frac{\omega_s \, 2(4\pi)^3 h^2 v}{G_o^2 f_1(\theta) f_2(\theta,\phi) P_t \lambda^3} \qquad (3\text{-}3)$$

where

σ_o = backscatter coefficient
ω_s = averaged return power
h = aircraft height
v = relative velocity
P_t = transmitted power
G_o = antenna gain
λ = signal wavelength
$f(\ )$ = antenna paterns

Since all other values can be held constant for a given length of time, the variance of the calculated signal

mean from the true mean will be equivalent to that of the averaged signal value plus noise, thus,

$$\delta\sigma_o = \delta\omega_s + \bar{n}$$

where $\delta\sigma_o$ = variance of the obtained backscatter coefficient from its true value

$\delta\omega_s$ = variance of the averaged backscattered power from its true value

$\bar{n}$ = averaged noise

The averaged noise will be assumed to be small compared with the signal, therefore,

$$\delta\sigma_o \approx \delta\omega_s$$

The return signal will be the result of transmitted pulses thus giving the effect of the return signal being sampled at the transmitted pulse rate. The Central Limit Theorem implies that the amplitude distribution of a sampled signal being averaged can be considered Gaussian. Therefore, the variance of the averaged power from its true mean will be determined using statistics involving Gaussian distributions

Detection

Consider the case where the return signal is mixed with another frequency, passed through a low pass filter, and detected with a linear detector, as shown in Fig. III-2. The spectrum of the signal will change as shown in Fig. III-3.

The spectral density of the output of the linear detector, $S_y(f)$, is evaluated from the input spectral density $S_x(f)$, where

$$S_x(f) = \begin{cases} A & \text{when } |f| \leq \tfrac{1}{2}\Delta f_d \\ 0 & \text{otherwise} \end{cases} \qquad (3\text{-}4)$$

where A = amplitude
Δf_d = doppler frequency used to define ground area
$\delta(f)$ = impulse function

and [22]

$$S_y(f) = \frac{\sigma_x^2}{2\pi}\delta(f) + \frac{1}{4}S_x(f) + \frac{1}{4\pi\sigma_x^2}\int_{-\infty}^{\infty} S_x(f')\,S_x(f-f')\,df' \qquad (3\text{-}5)$$

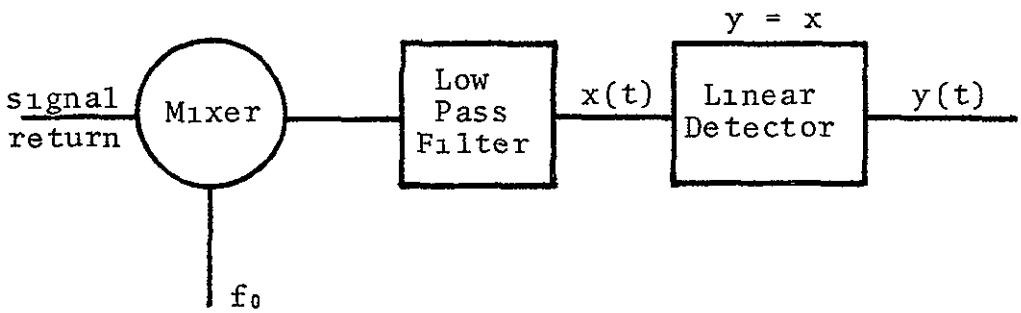

FIG. III-2 RETURN SIGNAL CIRCUIT

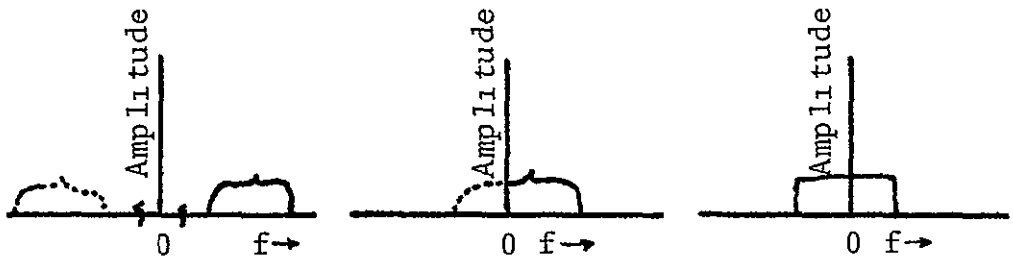

f - frequency

FIG. III-3

SPECTRAL CHANGE IN RETURN SIGNAL CIRCUIT

The variance, σ_x^2, of $S_x(f)$ is the area under its spectral density curve.

$$\sigma_x^2 = \int_{-\infty}^{\infty} S_x(f)\, df = 2 \int_{0}^{\frac{1}{2}\Delta f_d} A\, df = A \Delta f_d \tag{3-6}$$

Substituting this value for σ_x^2, $S_y(f)$ becomes

$$S_y(f) = \frac{A \Delta f_d}{2\pi} \delta(f) + \frac{1}{4\pi A \Delta f_d} \int_{-\infty}^{\infty} S_x(f')\, S_x(f-f')\, df' + \frac{1}{4} S_x(f) \tag{3-7}$$

The last term of the output spectral density equation is the convolution of the input spectral density. Thus,

$$\int_{-\infty}^{\infty} S_x(f')\, S_x(f-f')\, df' = \begin{cases} A^2 \Delta f_d \left(1 - \frac{|f|}{\Delta f_d}\right) & \text{when } |f| \le \Delta f_d \\ 0 & \text{otherwise} \end{cases}$$

Substituting this into eq. (3-7), $S_y(f)$ is finally arrived at in terms of frequency, f, and amplitude, A.

$$S_y(f) = \frac{A\Delta f_d}{2\pi}\delta(f) + \begin{cases} A/4 & \text{when } |f| \le \tfrac{1}{2}\Delta f_d \\ 0 & \text{otherwise} \end{cases} + \begin{cases} A^2\Delta f_d\left(1 - \frac{|f|}{\Delta f_d}\right) & \text{when } |f| \le \Delta f_d \\ 0 & \text{otherwise} \end{cases} \qquad (3\text{-}8)$$

The spectral density after linear detection, $S_y(f)$, will appear as shown in Fig. III-4.

The autocorrelation function, $R_y(T)$, which is used to determine the amount of independence between two parts of the detected signal, is obtained by taking the Fourier cosine transform of the spectral density $S_y(f)$ [23].

$$R_y(\tau) = \int_{-\infty}^{\infty} S_y(f)\cos(2\pi f \tau)\, df \qquad (3\text{-}9)$$

where τ = a time difference variable

By substituting eq. (3-8) into eq. (3-9) the auto-correlation function becomes

$$R_y(T) = \frac{A\,\Delta f_d}{2\pi} + 2\int_0^{\frac{1}{2}\Delta f_d} \frac{A}{4}\cos(2\pi f T)\,df + 2\int_0^{\Delta f_d} \frac{A}{4\pi}\left(1 - \frac{f}{\Delta f_d}\right)\cos(2\pi f T)\,df \tag{3-10}$$

Integrating eq (3-10), using integration by parts, $R_y(T)$ is derived as

$$R_y(T) = \frac{A\,\Delta f_d}{2\pi} + \frac{A}{2}\,\frac{\sin \pi \Delta f_d T}{2\pi T} + \frac{A}{2\pi}\,\frac{\sin 2\pi \Delta f_d T}{2\pi T} - \frac{A}{2\pi\,\Delta f_d}\int_0^{\Delta f_d} f\cos(2\pi f T)\,df$$

$$= \frac{A\,\Delta f_d}{2\pi} + \frac{A}{2}\,\frac{\sin \pi \Delta f_d T}{2\pi T} + \frac{A - A\cos 2\pi \Delta f_d T}{(2\pi)^3\,\Delta f_d\,T^2} \tag{3-11}$$

The trigometric identity for $\sin^2\theta$ is used to simplify $R_y(T)$

$$2\sin^2\theta = 1 - \cos 2\theta \tag{3-12}$$

The final result for the autocorrelation function of the signal after linear detection is therefore

$$R_y(T) = \frac{A\Delta f_d}{2\pi} + \frac{A \sin \pi \Delta f_d T}{4\pi T} + \frac{A \sin^2 \pi \Delta f_d T}{(2\pi)^2 \pi \Delta f_d T^2} \tag{3-13}$$

The first term of $R_y(T)$ is the square of the mean value of y(t) (i.e. η_y^2) The rest of $R_y(T)$ evaluated at T = 0 gives the variance, σ_y^2.

$$\eta_y^2 = \frac{A\Delta f_d}{2\pi}$$

$$\sigma_y^2 = \frac{A\Delta f_d}{4} + \frac{A\Delta f_d}{4\pi} = \frac{\sigma_x^2}{4}\left(1 + \frac{1}{\pi}\right) \tag{3-14}$$

This follows from the fact that $R_y(0)$ is the mean square value of the signal, y(t), transmitted from the linear detector. This value of $R_y(T)$ is obtained by assuming that the mean value of the input signal X(t) is zero, and that X(t) is a sample function of a real Gaussian random process.

In light of the criteria concerning the return signal, this assumption may at first seem erroneous Therefore, an insight into the statistics of the return signal will be useful The amplitude of the return signal is

Rayleigh distributed. Let the signal be interpreted as the sampled return of a continuous wave (CW) system instead of the actual return of the transmitted interrupted continuous wave (ICW) signal. Then, the amplitude and samples of the signal would appear as shown in Fig. III-5.

The amplitude distribution of the sampled signal is Rayleigh distributed. However, the distribution of the mean value obtained by averaging N independent samples will tend to become Gaussian as the number of independent samples N increases.

$$A_N = \frac{a_1 + a_2 + \cdots + a_N}{N}$$

where A_N = the sampled mean
a_i = the ith voltage sample
N = the total number of samples

As N increases, the sampled mean will approach the true mean, η, of the signal, and the probability distribution of the sampled mean, $f_{A_N}(x)$, tends to be Gaussian regardless of the probability distribution of each independent sample This is a statement of the Central Limit Theorem which is valid for independent samples having a finite mean, η, and a finite variance, σ^2 [24]

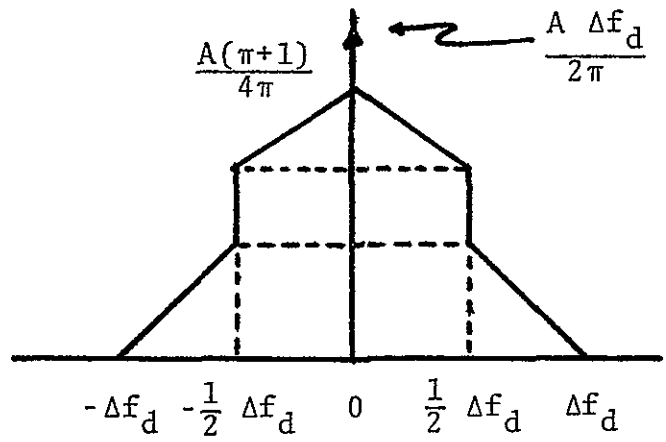

FIG III-4 SPECTRAL DENSITY AFTER LINEAR DETECTION

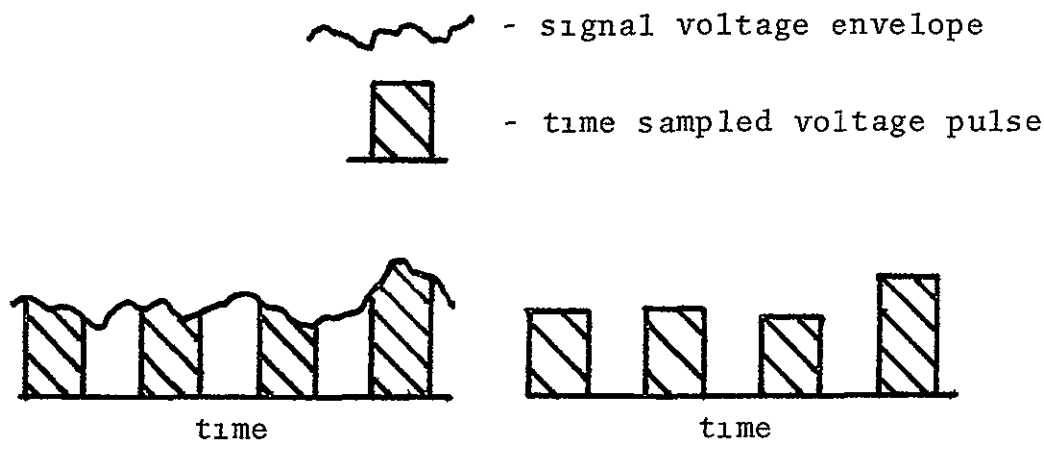

FIG III-5 SAMPLE AMPLITUDES

Gaussian techniques are valid for determining the autocorrelation $R_y(T)$ of the return signal pulses. It must be noted though, that the probability density of the sampled mean is not truly Gaussian unless N approaches infinity. For all practical purposes, considering a Rayleigh distributed input amplitude, the sampled mean can be considered Gaussian after about ten independent samples [25]

In using Gaussian techniques, trouble arises due to the mean value of the incoming signal, η_x, not being identically zero, an assumption necessary in determining the equation for $S_y(f)$ as a function of $S_x(f)$. This can be corrected for by placing a stringent specification on the calculated $R_y(T)$ as to what constitutes an independent sample The qualifications for sample independence are arbitrary but they must be strong enough to account for any error which will arise due to the inherent incorrect assumption made in order to calculate $R_y(T)$.

Before these qualifications are stated, the autocorrelation function will be converted to a more convenient form A new function, $K_y(T)$, is formed by subtracting the constant term from $R_y(T)$.

$$K_y(T) = R_y(T) - \frac{A \Delta f_d}{2\pi} \qquad (3\text{-}15)$$

Substituting for $R_y(T)$, $K_y(T)$ becomes

$$K_y(T) = \frac{A \sin \pi \Delta f_d T}{4\pi T} + \frac{A \sin^2 \pi \Delta f_d T}{(2\pi)^2 \pi \Delta f_d T^2} \qquad (3\text{-}16)$$

To rid $K_y(T)$ of the amplitude value A, the function $K_y(T)$ is divided by its initial value, $K_y(T = 0)$, thus obtaining a normalized value $\rho(T)$

$$\rho(T) = \frac{K_y(T)}{K_y(0)}$$

$$K_y(0) = \frac{A \Delta f_d (1 + \frac{1}{\pi})}{4} \qquad (3\text{-}17)$$

The equation $\rho(T)$ finally becomes

$$\rho(T) = \frac{\sin \pi \Delta f_d T}{\pi \Delta f_d T (1 + \frac{1}{\pi})} + \frac{\sin^2 \pi \Delta f_d T}{(2\pi)^2 \Delta f_d^2 T^2 (\pi + 1)} \qquad (3\text{-}18)$$

In some notation, $K_y(T)$ is called the autocovariance function, and $\rho(T)$ is called the normalized autocovariance function, which has also been called the autocorrelation function [26]

The autocorrelation $\rho(T)$ goes to zero at

$$\Delta f_d \tau = 1, 2, 3, \quad , n, \qquad \text{Therefore } \tau_n = \frac{n}{\Delta f_d}$$

A good criteria for independence is for the auto-correlation function to be less than one-tenth after a certain time T. For convenience, the criteria will be set as

$$\rho(T) \leq \frac{1}{\pi^2} \quad \text{for all } \tau > T_1$$

and

$$\rho(T_2) = 0 \quad \text{where } T_2 > T_1$$

Using these conditions,

$$\rho(T_n) = 0 = \frac{\sin(n\pi)}{n(\pi+1)} + \frac{\sin^2(n\pi)}{(2\pi)^2 n^2(\pi+1)} \qquad (3\text{-}19)$$

and

$$\rho(T) \leq \frac{1}{\pi^2} \quad \text{when } \tau > T_n$$

The criteria n = 3 will satisfy these two conditions.

$$\tau = \frac{3}{\Delta f_d} = t_{IS} \tag{3-20}$$

where t_{IS} = time between independent samples

Under this criteria, sampling at every $\frac{3}{\Delta f_d}$ seconds will give a set of independent samples. If the sampling time is slightly greater, two adjacent samples will have some correlation which is less than $\frac{1}{\pi^2}$ which also satisfies the independence criteria If the sampling time is less than $\frac{3}{\Delta f_d}$ seconds, only the string of samples being equal to or greater than $\frac{3}{\Delta f_d}$ seconds apart can be considered independent

The first sample is the first independent sample. Therefore, at $\frac{3}{\Delta f_d}$ seconds later, the second independent sample can exist, for $2 \cdot \frac{3}{\Delta f_d}$, the third, and so on

Sampled Variance of the Mean

The amplitude distribution of each pulse received is random in a Rayleigh manner. The Rayleigh distribution has the mean and variance shown.

$$f(x) = \frac{x}{\alpha^2} e^{-\frac{x^2}{2\alpha^2}} U(x) \tag{3-21}$$

mean

$$\eta = \int_{-\infty}^{\infty} x\, f(x)\, dx = \int_{0}^{\infty} \frac{x^2}{\alpha^2} e^{-\frac{x^2}{2\alpha^2}}\, dx$$

$$= \alpha \sqrt{\frac{\pi}{2}} \qquad (3\text{-}22)$$

where α = value where f(x) is maximum
$U(x)$ = unit step function

variance

$$\sigma^2 = \int_{-\infty}^{\infty} x^2 f(x)\, dx - \eta^2$$

$$= \left(2 - \frac{\pi}{2}\right) \alpha^2 \qquad (3\text{-}23)$$

For independent samples, a_1, the sampled mean A_N, will be

$$A_N = \frac{a_1 + a_2 + \cdots + a_N}{N}$$

For independent samples the variance, σ^2_i, is

$$\sigma^2_{a_1 + a_2 + \cdots + a_N} = \sigma^2_{a_1} + \sigma^2_{a_2} + \cdots + \sigma^2_{a_N}$$

For any signal from the same patch of ground, every return pulse will have the same variance with identical Rayleigh distributions. Thus,

$$\sigma_{a_1}^2 = \sigma_{a_2}^2 = \cdots = \sigma_{a_N}^2 = \sigma^2$$

and

$$\sigma_{A_N}^2 = \frac{\sigma_{a_1}^2 + \sigma_{a_2}^2 + \cdots + \sigma_{a_N}^2}{N^2} = \frac{N\sigma^2}{N^2} = \frac{\sigma^2}{N} \tag{3-24}$$

With an increasing number of independent samples, the variance of the sampled mean goes to zero, i.e. the sampled mean approaches the true or Rayleigh distribution mean

From Tchebycheff's Inequality, the probability P that A_N is within a certain range is given by [27]

$$P\{\eta - c\eta \leq A_N \leq \eta + c\eta\} \geq \frac{\sigma^2}{N c^2 \eta^2} \tag{3-25}$$

Since the incoming signal, x(t) is Rayleigh distributed, the ratio of the mean squared, η^2_x, to variance, σ^2_x, is

$$\frac{\sigma_x^2}{\eta_x^2} = \frac{(2-\frac{\pi}{2})\alpha^2}{\frac{\pi}{2}\alpha^2} = \frac{4-\pi}{\pi} = .272 \qquad (3\text{-}26)$$

Thus,

$$P\{\eta_x(1-c) \leq A_N \leq \eta_x(1+c)\} \geq 1 - \frac{.272}{Nc^2} \qquad (3\text{-}27)$$

$$\geq 1 - K$$

where

$$K = \frac{.272}{Nc^2}$$

Consider finding the probability that the value A_N is within ± 3db of η_x where A_N is the averaged value of the return envelope voltage V_s.

$$3\ db = 20 \log \frac{\Delta A_N}{\eta_x} \qquad \Delta A_N = \eta_x(1+c) \qquad (3\text{-}28)$$

This requires that

$$\frac{\Delta A_N}{\eta_x} = \frac{(1+c)\eta_x}{\eta_x} = (1+c) \approx 1.413 \qquad (3\text{-}29)$$

Therefore, solving for c,

$$c = .413$$

$$K = \frac{.272}{N(.413)^2} = \frac{1.59}{N} \qquad (3\text{-}30)$$

To be greater than 99% certain that A_N is within 3db of η_x, i.e. 1-K = 99, K = .01 = $\frac{1\ 59}{N}$, therefore N = 159 Thus, 159 independent samples are needed Consider, the probability that A_N is within ±1db of η_x. For this,

$$1db = 20 \log \frac{\Delta A_N}{\eta_x}$$

$$= 20 \log (1+c)$$

Thus,

$$1+c = 1.121$$

$$c = .121 \qquad (3\text{-}31)$$

Therefore

$$K = \frac{.272}{N(.121)^2} = \frac{18.6}{N}$$

To be greater than 90% certain that A_N is within ±1db of η_x, using eq. (3-27) and eq (3-31)

$$1 - K = .90 \Rightarrow K = .10$$

$$K = .10 = \frac{18.6}{N} \Rightarrow 186 = N$$

To be greater than 99% certain that A_N is within ±1db of η_x

$$1 - K = .99 \Rightarrow K = .01$$

$$K = .01 = \frac{18.6}{N} \Rightarrow N = 1860$$

Consider scanning a cell area having a change in doppler frequency of at least 280 Hz. An independent sample will occur in the time specified by eq. (3-20)

$$t_{1s} = \frac{3}{\Delta f_d} = \frac{3}{280} = .01071 \text{ seconds}$$

In viewing the same cell area for 0.2 seconds, which is the cell viewing time for the scatterometer system described in Chapter II, the number of independent samples will be as shown

$$N = \frac{T}{t_{is}} + 1 = \frac{.2}{.01071} + 1$$

$$= 19 \qquad (3\text{-}32)$$

Thus, 19 independent samples are received and the probability shown in Table III-1 is derived with N = 19 from the probability equation, eq (3-27)

$$P\{\eta_x(1-c) \le A_N \le \eta_x(1+c)\} \ge 1 - \frac{.272}{c^2 N} = 1 - \frac{.0143}{c^2}$$

Table III-1 shows that for 1000 values of V_s obtained from viewing for 0.2 seconds, cells having a change in doppler frequency of 280 Hz, at least 995 of the values are correct to within ±8 6 db of the actual or true value, η_x, at least 990 of them are correct within ±6.82 db, at least 980 are correct within ±5 34 db, etc

The Tchebycheff Inequality
Using 19 Independent Samples
and Rayleigh Distributed Signal

Percent of Certainty	A_N Within $\pm K$ db of η_x	Value of C
0 0%	0.98	.1195
10%	1.04	.126
90%	2.78	.378
95%	3.72	.535
96%	4.04	.598
97%	4 56	.690
98%	5.34	.845
99%	6 82	1 195
99.5%	8.60	1.691

TABLE III-1 PROBABILITY LIST

Since, for the conditions stated, no averaged value can be said to be correct to within less than ±0.98 db of the true value, this constitutes the lower limit for accuracy

The number of independent samples is given by

$$N = \frac{T}{t_{1s}} + 1 = \frac{T \Delta f_d}{3} + 1 \qquad (3\text{-}33)$$

where T = viewing time
Δf_d = doppler frequency change across a cell
t_{1s} = one independent sample time period

Therefore, either an increase in T or an increase in Δf_d would improve the mean determinance of V_s for this system The above equation for N holds assuming the criteria that sampling occurs once every $t_{1.s}$ seconds. For sampling faster than this, equation (3-33) reduces to

$$N = \frac{T}{t_{1s}} = \frac{T \Delta f_d}{3} \qquad (3\text{-}34)$$

Due to this faster sampling, one independent sample will exist for every period duration of $t_{1\ s}$ seconds. Thus, in averaging, numerous pulses will represent one independent sample

There exists another method for finding the prob-

ability, P, that a value z lies within a certain region (a,b) on the density curve $f_z(x)$, is given by [28]

$$P\{a \le z \le b\} = \int_a^b f_z(x)\,dx$$

Using the Central Limit Theorem, the distribution of the sampled mean, A_N, about the mean, η_x, of the incoming signal, x(t), will be Gaussian Thus, using the definition of probability, the probability that A_N will be within a certain db range of the mean will be

$$P\{\eta_x(1-c) \le A_N \le \eta_x(1+c)\} = \int_{\eta_x(1-c)}^{\eta_x(1+c)} \frac{1}{\sqrt{2\pi\,\sigma_{A_N}^2}}\, e^{-\frac{(x-\eta_x)^2}{2\sigma_{A_N}^2}}\,dx$$

$$= \int_{\eta_x(1-c)}^{\eta_x(1+c)} f_{A_N}(x)\,dx \qquad (3\text{-}35)$$

The db range is given by

$$db = \pm 20 \log \frac{\Delta A_N}{\eta_x} = \pm 20 \log(1+c) \qquad (3\text{-}36)$$

The probability integral is now reduced to

$$P\{\eta_\chi(1-c) \le A_N \le \eta_\chi(1+c)\} = \frac{1}{\sqrt{2\pi}} \int_{-b}^{b} e^{-\frac{z^2}{2}} dz \qquad (3\text{-}37)$$

where

$$z = \frac{\chi - \eta_\chi}{\sigma_{A_N}} \qquad b = \frac{c\,\eta_\chi}{\sigma_{A_N}}$$

This is further reduced using the quantity called the error function, erf [29].

$$\operatorname{erf} \chi = \frac{1}{\sqrt{2\pi}} \int_{0}^{\chi} e^{-\frac{z^2}{2}} dz \qquad (3\text{-}38)$$

The probability of A_N being within a certain range is now given by

$$P = 2 \operatorname{erf} b = 2 \operatorname{erf} \frac{c\,\eta_\chi}{\sigma_{A_N}} \qquad (3\text{-}39)$$

The db range for this probability can readily be evaluated from the above equation The variance, $\sigma^2_{A_N}$, and mean, η_x, values are the same as given before

$$\sigma^2_{A_N} = \frac{\sigma_i^2}{N} = \frac{\frac{4-\pi}{2}\alpha^2}{N} \qquad \eta_x = \sqrt{\frac{\pi}{2}}\,\alpha$$

$$\frac{\eta_x}{\sigma_{A_N}} = \sqrt{N}\sqrt{\frac{\pi}{4-\pi}} = \sqrt{N}\ 1.913 \tag{3-40}$$

Therefore the probability will be

$$P = 2\,\mathrm{erf}\ c\sqrt{N}\ 1.913 \tag{3-41}$$

For A_N to be within ±2db of η_x, the requirement is that C = .260

$$P = 2\,\mathrm{erf}\,(.260)(1.913)\sqrt{N} \tag{3-42}$$

when N = 4, P = 68%
N = 9, P = 86%
N = 18, P = 96%
N = 25, P = 98%
N = 36, P = 99.3%

For A_N to be within ±1db of η_x, the requirement is that C = 121

$$P = 2\,\mathrm{erf}\,(.121)(1.913)\sqrt{N} \qquad (3\text{-}43)$$

when N = 4, P = 35%
N = 9, P = 50%
N = 18, P = 67%
N = 25, P = 75%
N = 36, P = 83%

Determinance of the Mean Power Values

The previous calculations have determined the variance of the sampled and time averaged voltage mean value from the true envelope voltage mean value, η_x. In determining a value such as the backscatter coefficient, a value for the mean power is required Power is a function of the envelope voltage squared.

$$P = \frac{V^2}{R}$$

where V = voltage
P = power
R = resistance - this value is made to equal one

A mean power value W_s can be derived by squaring the voltage mean value A_N.

$$W_S = (A_N)^2 \qquad A_N = \sum_{i=1}^{N} \frac{a_i}{N} \tag{3-44}$$

where a_i = the ith independent voltage sample

Another way to obtain a mean power value is by averaging the power values.

$$B_N = \sum_{i=1}^{N} \frac{(a_i)^2}{N} \tag{3-45}$$

where it can be shown that

$$B_N \geq (A_N)^2$$

As N increases, confidence $B_N \rightarrow$ confidence $(A_N)^2$, therefore, the statistics of B_N will be used to evaluate the statistics of $(A_N)^2$. This will give approximate values only. The statistics of $(A_N)^2$ are given after the statistics of B_N

Let

$$R = X^2$$

where $X = a_i$ = independent voltage sample

The density of X, $f_x(x)$, is Rayleigh and given by

$$f_x(x) = \frac{x}{\alpha^2} e^{-\frac{x^2}{2\alpha^2}} U(x)$$

$$\eta_x = \sqrt{\frac{\pi}{2}}\,\alpha \qquad \sigma_x^2 = \left(2 - \frac{\pi}{2}\right)\alpha^2 \tag{3-46}$$

The density of R, $f_R(y)$, is found as shown [30].

$$f_R(y) = \frac{1}{2\sqrt{y}}\left[f_x(\sqrt{y}) + f_x(-\sqrt{y})\right] U(y) \tag{3-47}$$

Substituting eq. (3-46), f_R becomes

$$f_R(y) = \frac{1}{2\sqrt{y}}\left[\frac{\sqrt{y}}{\alpha^2} e^{-\frac{y}{2\alpha^2}} U(\sqrt{y}) + \frac{-\sqrt{y}}{\alpha^2} e^{-\frac{y}{2\alpha^2}} U(-\sqrt{y})\right] U(y) \tag{3-48}$$

but

$$U(-\sqrt{y}) = 0$$

since the unit step U(c) is defined as zero for negative c. Therefore,

$$f_R(y) = \frac{1}{2\alpha^2} e^{-\frac{y}{2\alpha^2}} \; U(y). \tag{3-49}$$

The mean and variance of R can now be found

mean

$$\eta_R = E\{y\} = \int_{-\infty}^{\infty} y \, f_r(y) \, dy = \frac{1}{2\alpha^2} \int_0^{\infty} y \, e^{-\frac{y}{2\alpha^2}} dy$$

$$= 2\alpha^2 = \frac{4}{\pi} \eta_x^2$$

$$E\{y^2\} = \int_{-\infty}^{\infty} y^2 f(y) \, dy$$

$$= \frac{1}{2\alpha^2} \int_0^{\infty} y^2 e^{-\frac{y}{2\alpha^2}} \, dy$$

$$= 8\alpha^4 \tag{3-50}$$

variance

$$\sigma_R^2 = E\{y^2\} - E^2\{y\}$$

$$= 8\alpha^4 - (2\alpha^2)^2$$

$$= 4\alpha^4 \tag{3-51}$$

where η_R = mean value of R
σ_R^2 = variance of R

Using the Central Limit Theorem, the density function, $f_{B_N}(z)$, of the average B_N becomes Gaussian as N increases

$$f_{B_N}(z) = \frac{1}{\sqrt{2\pi\sigma_{B_N}^2}} e^{-\frac{(z-\eta_R)^2}{2\sigma_{B_N}^2}} \tag{3-52}$$

where

$$\sigma_{B_N}^2 = \frac{\sigma_i^2}{N} = \frac{4\alpha^4}{N}$$

$$\sigma_i^2 = \sigma_R^2$$

Thus, the level of confidence or percent of probability that B_N is within a certain db range of the true mean is, in the manner it was for A_N in eq. (3-39), given by

$$P\{\eta_y(1-c) \le B_N \le \eta_y(1+c)\} = 2\,\mathrm{erf}\,\frac{c\,\eta_R}{\sigma_{B_N}} \tag{3-53}$$

Using the statistics derived for B_N, it follows that

$$\frac{\eta_R}{\sigma_{B_N}} = \frac{2\alpha^2}{\frac{2\alpha^2}{\sqrt{N}}} = \sqrt{N} \tag{3-54}$$

and

$$db = \pm 10 \log (1+c)$$

For B_N to be within ±1db of η_y, the requirement is that C = .260, giving the probability shown

$$P = 2\,erf(.260)\sqrt{N} \tag{3-55}$$

when N = 2, P = 40%
N = 9, P = 56%
N = 18, P = 73%
N = 25, P = 80%
N = 36, P = 88%
N = 49, P = 93%

The statistics of $(A_N)^2$ are summarized below in the same manner that those of B_N were presented Now, from eq. (3-44),

$$A_N = \sum_{i=1}^{N} \frac{a_i}{N}$$

By the Central Limit Theorem, the density A_N, $f_{A_N}(x)$, is Gaussian

$$f_{A_N} = \frac{1}{\sqrt{2\pi\,\sigma_{A_N}^2}}\; e^{-\frac{(x-\eta_{A_N})^2}{2\sigma_{A_N}^2}} \qquad (3\text{-}56)$$

Let

$$S = (A_N)^2$$

$$\eta_{A_N} = \eta$$

$$\sigma_{A_N}^2 = \sigma$$

now, the density, $f_S(y)$, of S is, as in eq. (3-47), given by

$$f_S(y) = \frac{1}{2\sqrt{y}} \left[f_{A_N}(\sqrt{y}) + f_{A_N}(-\sqrt{y}) \right] U(y) \qquad (3\text{-}57)$$

Substituting eq (3-56) into this equation, $f_s(y)$ becomes

$$f_s(y) = \frac{1}{\sqrt{8\pi y \sigma^2}} \left[e^{\frac{-(\sqrt{y}-\eta)^2}{2\sigma^2}} + e^{\frac{-(\sqrt{y}+\eta)^2}{2\sigma^2}} \right] U(y) \qquad (3\text{-}58)$$

Squaring the exponent and separating parts, $f_s(y)$ becomes

$$f_s(y) = \frac{1}{\sqrt{8\pi y \sigma^2}} e^{-\frac{(y+\eta^2)}{2\sigma^2}} \left[e^{\frac{\sqrt{y}\eta}{\sigma^2}} + e^{-\frac{\sqrt{y}\eta}{\sigma^2}} \right] U(y) \qquad (3\text{-}59)$$

$$= \frac{e^{-\frac{\eta^2}{2\sigma^2}}}{\sqrt{2\pi\sigma^2}} \left[\frac{1}{\sqrt{y}} e^{-\frac{y}{2\sigma^2}} \cdot \cosh \frac{\sqrt{y}\eta}{\sigma^2} U(y) \right] \qquad (3\text{-}60)$$

The mean value, η_s, of $f_s(y)$ is given by

$$\eta_s = \int_{-\infty}^{\infty} y f_s(y) \, dy \qquad (3\text{-}61)$$

Substituting in $f_s(y)$, η_s now becomes

$$\eta_s = \frac{e^{-\frac{\eta^2}{2\sigma^2}}}{\sqrt{2\pi\sigma^2}} \int_0^\infty \sqrt{y}\, e^{-\frac{y}{2\sigma^2}} \cosh\left(\frac{\sqrt{y}\,\eta}{\sigma^2}\right) dy$$

$$= \frac{e^{-\frac{\eta^2}{2\sigma^2}}}{\sqrt{2\pi\sigma^2}} \; 2\sqrt{\frac{\pi}{2}} \left(\sigma^3 + \eta^2\sigma\right) e^{\frac{\eta^2}{2\sigma^2}}$$

$$= \sigma^2 + \eta^2$$

$$= \eta^2\left(\frac{\sigma^2}{\eta^2} + 1\right) \qquad (3\text{-}62)$$

The mean value of $(A_N)^2$, η_s, finally becomes

$$\eta_s = \eta_{A_N}^2 \left(\frac{4-\pi}{N\pi} + 1\right) \qquad (3\text{-}63)$$

Finding the percent of certainty or level of confidence that $(A_N)^2$ is within $\pm K$ db of η_s is accomplished by performing the following calculations The db range in terms of c is given by

$$K\ \text{db} = \pm 10 \log (1+c) \qquad (3\text{-}64)$$

The probability P is, as shown in eq. (3-35)

$$P\left\{\eta_s(1-c) \le (A_N)^2 \le \eta_s(1+c)\right\} = \int_{\eta_s(1-c)}^{\eta_s(1+c)} f_s(y)\,dy \qquad (3\text{-}65)$$

Substituting $f_s(y)$ in eq. (3-58), P becomes

$$P = \frac{1}{\sqrt{8\pi\sigma^2}} \int_{\eta_s(1-c)}^{\eta_s(1+c)} \frac{1}{\sqrt{y}} \left[e^{\frac{-(\sqrt{y}-\eta)^2}{2\sigma^2}} + e^{-\frac{(\sqrt{y}+\eta)^2}{2\sigma^2}} \right] dy \qquad (3\text{-}66)$$

for integration purposes, let $y = x^2$ and $dy = 2xdx$.

Therefore,

$$P = \frac{1}{\sqrt{2\pi\sigma^2}} \int_{\sqrt{\eta_s(1-c)}}^{\sqrt{\eta_s(1+c)}} e^{-\frac{(x-\eta)^2}{2\sigma^2}} + e^{-\frac{(x+\eta)^2}{2\sigma^2}}\,dx \qquad (3\text{-}67)$$

now, let

$$z = \frac{x+\eta}{\sigma} \qquad dx = \sigma\,dz$$

and

$$W = \frac{x-\eta}{\sigma} \qquad dx = \sigma\, dw$$

The level of confidence now becomes

$$P = \frac{1}{\sqrt{2\pi}} \int_{\frac{\sqrt{\eta_s(1-c)}+\eta}{\sigma}}^{\frac{\sqrt{\eta_s(1+c)}+\eta}{\sigma}} e^{-\frac{z^2}{2}}\, dz + \frac{1}{\sqrt{2\pi}} \int_{\frac{\sqrt{\eta_s(1-c)}-\eta}{\sigma}}^{\frac{\sqrt{\eta_s(1+c)}-\eta}{\sigma}} e^{-\frac{w^2}{2}}\, dw \tag{3-68}$$

Using the error function definition of eq. (3-38), P becomes

$$P = \operatorname{erf}\left(\frac{\sqrt{\eta_s(1+c)}+\eta}{\sigma}\right) - \operatorname{erf}\left(\frac{\sqrt{\eta_s(1-c)}+\eta}{\sigma}\right)$$

$$+ \operatorname{erf}\left(\frac{\sqrt{\eta_s(1+c)}-\eta}{\sigma}\right) + \operatorname{erf}\left(\frac{\sqrt{\eta_s(1-c)}-\eta}{\sigma}\right) \tag{3-69}$$

Substituting the value for η_s in eq (3-62), P becomes

$$P = \operatorname{erf}\left\{\frac{\eta}{\sigma}\left(\sqrt{\left(\frac{\sigma^2}{\eta^2}+1\right)(1+C)}+1\right)\right\} - \operatorname{erf}\left\{\frac{\eta}{\sigma}\left(\sqrt{\left(\frac{\sigma^2}{\eta^2}+1\right)(1-C)}+1\right)\right\} + \operatorname{erf}\left\{\frac{\eta}{\sigma}\left(\sqrt{\left(\frac{\sigma^2}{\eta^2}+1\right)(1+C)}-1\right)\right\} - \operatorname{erf}\left\{\frac{\eta}{\sigma}\left(\sqrt{\left(\frac{\sigma^2}{\eta^2}+1\right)(1-C)}-1\right)\right\} \tag{3-70}$$

For $(A_N)^2$ to be within ±1db of η_s, C = 260 as found from eq. (3-64). Let N = 36

$$\frac{\eta}{\sigma} = \sqrt{\frac{36\pi}{4-\pi}} = 11.5$$

$$\frac{\sigma^2}{\eta^2} = .758 \times 10^{-2} \tag{3-71}$$

The probability that $(A_N)^2$ is within ±1db of η_s for N = 36 is

$$P = \operatorname{erf}(22.4) - \operatorname{erf}(21.4) + \operatorname{erf}(1.39) - \operatorname{erf}(-1.61) \tag{3-72}$$

For large β, i.e. β > 5,

$$\operatorname{erf}\ \beta \approx \frac{1}{2} \qquad \operatorname{erf}(-\beta) = -\operatorname{erf}\beta$$

therefore erf (22.4) $\cong$ erf (21.4) and the probability equation reduces to

$$P = erf(1.39) + erf(1.61)$$

$$= 86\% \tag{3-73}$$

which is approximately the probability for B_N when C = .260 and N = 36.

Now consider the probability that $(A_N)^2$ is within ±1db of η_s. For N = 49 and C = .260, the ratio $\frac{\eta}{\sigma}$ becomes

$$\frac{\eta}{\sigma} = \sqrt{\frac{49\pi}{4-\pi}} = 13.4$$

$$\frac{\sigma^2}{\eta^2} = 5.66 \times 10^{-3} \tag{3-74}$$

Therefore the probability becomes, with erf (a > 5)= erf (b > 5)

$$P = erf(1.62) + erf(1.88)$$

$$= 91\% \tag{3-75}$$

Summary

The results obtained apply to the scanning scatterometer described in Chapter II. The scatterometer reception of the Rayleigh distributed voltage return signal is shown to contain 18 independent samples during the 0 2 second integration time for a doppler bandwidth of 280 Hz The variance of the backscatter coefficient from the true value was determined in terms of db variance and level of confidence, and their dependence on integration time was calculated A comparison of the average voltage squared, $(A_N)^2$, and the average power level, B_N, shows that these two quantities do not tend towards the same values even though their confidence levels are nearly identical.

The results obtained by the scatterometer, averaging only 18 independent samples, i e. 0 2 seconds and 280 Hz, are shown to be inadequate due to the low level of confidence. Adequate results can be obtained by increasing the number of independent samples to 49 This is accomplished by either increasing Δf_d, the doppler bandwidth, or the viewing time for a cell. Doing such would cause improvements in the scatterometer accuracy for determining the scattering coefficient, but the results of doing so would decrease the resolution.

CHAPTER IV

FREQUENCY AVERAGING

Frequency Agility

Most radar scatterometers utilize monochromatic transmission. There exists the possibility that frequency agility or panchromaticity may inhance a systems ability to determine the scattering coefficient

A frequency agile system works on the premise that there exists a frequency change, Δf_c, which, if implemented between pulses, would constitute independence between the two pulses. Thus, the transmitting frequency would be increased Δf_c between each pulse until the desired number of independent samples is reached However, there exists difficulties in using frequency agility The main problem can be seen by viewing the standard radar equation used in the scatterometer data normalizer to calculate the backscatter coefficient

$$\sigma_o = \frac{W_s \, 2(4\pi)^3 \, h^2 \, v}{P_t \, G_o^2 \, f_1(\theta) \, f_2(\theta,\phi) \, \lambda^3} \qquad (4\text{-}1)$$

The variation in σ_0 with respect to wavelength, λ, can vary from λ^{+2} to λ^{-6} dependent upon surface conditions [31]. For purposes of calculations, a σ_0 dependency of λ^{-3} will be assumed If in using frequency agility, the wavelength range difference would be six percent of the center frequency wavelength (i.e. $\Delta\lambda = .06\lambda$), the variation in σ_0 would be

$$\pm \delta\sigma_o = 1 - \frac{1}{\left(1 + \frac{\delta\lambda}{\lambda_o}\right)}$$

$$= .085 \qquad (4\text{-}2)$$

or

$$\delta\sigma_o = \pm .36 \text{ db} \qquad (4\text{-}3)$$

where $\delta\lambda$ = variance in center wavelength = $\pm 0.03\ \lambda_0$
λ_o = center wavelength
$\delta\sigma_o$ = variance in backscatter coefficient

Thus, a scatterometer having a transmitting center frequency of 13 3 GHz would have an inherent error of ±0.36 db with a frequency change of ±400 MHz. Whether or not such a large frequency variance is necessary will be shown later.

The Autocorrelation Function Vs. Frequency Agility

The autocorrelation for a low-pass spectral input to a linear detector has previously been calculated. This autocorrelation function holds for correlation between pulses having identical transmission frequencies. Pulses received having had different transmission frequencies will have a different autocorrelation function to determine independence between pulses of different frequencies.

Suppose that there exists a M pulse repetitive sequence in a frequency agile scatterometer, and that each succeeding pulse frequency is increased by Δf_c, such that each returning pulse constitutes an independent sample. Then, M independent samples would exist every $t_{i.s.}$ seconds. The interval $t_{i.s}$ is dependent upon the monochromatic autocorrelation function, and it designates time difference between pulses of identical frequencies necessary for those pulses to be considered independent. When the time necessary for the M pulse sequence is less than $t_{i\ s.}$ seconds, only one pulse at each specific frequency within each time period of $t_{i\ s}$ seconds will constitute an independent sample (see Fig. IV-1). Thus, when three pulses exist in the M pulse sequency, i e. M = 3, three independent samples exist every $t_{i\ s.}$ seconds

The frequency autocorrelation function of a back-scattered signal has been shown to be [32]

$$\rho(\Delta f) = \frac{\sin^2\left(\frac{2\pi L \sin\theta\ \Delta f}{c}\right)}{\left(\frac{2\pi L \sin\theta\ \Delta f}{c}\right)^2} \qquad (4\text{-}4)$$

where c = speed of light
$\rho(\Delta f)$ = frequency autocorrelation function
L = length of object being viewed
θ = angle of signal incident upon the object
Δf = frequency difference from one pulse to another

Independence between signals of different frequencies will be assumed to occur when the frequency autocorrelation function is less than one-tenth. For convience of calculations, independence will be defined as occurring when $\rho(\Delta f) \leq \frac{1}{\pi^2}$. Therefore, letting the denominator equal π^2, the calculation of Δf_c yields

$$\left(\frac{2\pi L \sin\theta\ \Delta f_c}{c}\right)^2 = \pi^2$$

$$\Delta f_c = \frac{c}{2L\sin\theta} = \frac{150\ \text{MHz}}{L\sin\theta} \qquad (4\text{-}5)$$

The ground length viewed, L, can be estimated using the diagram of Fig IV-2.

The doppler frequency value along the ground in the flight direction is given by

$$f_d = \frac{2v}{\lambda} \sin\theta = \frac{2vf}{c} \sin\theta \qquad (4\text{-}6)$$

where f_d = doppler frequency
v = aircraft velocity
f = transmitted frequency
c = speed of light
θ = angle of signal incident upon L

Holding velocity and frequency constant, the derivative of f_d will be

$$df_d = \frac{2vf}{c} \cos\theta \, d\theta \qquad (4\text{-}7)$$

For small $d\theta$, this equation can be approximated as

$$\Delta f_d = \frac{2vf}{c} \cos\theta \, \Delta\theta \qquad (4\text{-}8)$$

where Δf_d = doppler frequency shift contained along the distance L
$\Delta\theta$ = differential angle through which L is viewed

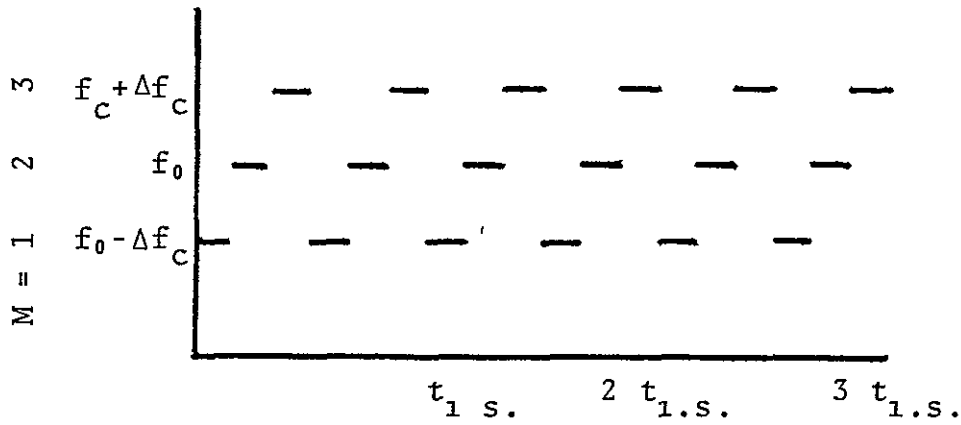

N = 1,2,3,. . .,4,5,6,. .,7,8,9,. . .

N = number of independent samples

FIG IV-1

EFFECTS OF FREQUENCY AGILITY UPON SAMPLE INDEPENDENCE

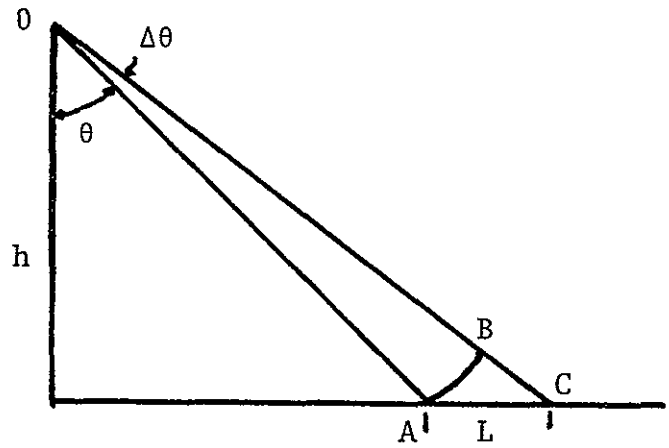

FIG. IV-2 SIGNAL TRANSMISSION PATH DIAGRAM

The radial distance, r, from 0 to A (see Fig. IV-2) is found by the relationship of a right triangle.

$$r = \frac{h}{\cos\theta} \tag{4-9}$$

where h = height above ground for aircraft
r = radial distance from aircraft to ground

For a small $\Delta\theta$, the arc AB can be considered a straight line. The arc has a length of $\overline{AB} = r\Delta\theta$. When the arc is considered as a straight line in the right triangle ABC, a relationship exists between L and $\Delta\theta$.

$$AB = r\Delta\theta = L\cos\theta \tag{4-10}$$

Substituting the relationship derived for r, the equation for $\Delta\theta$ becomes

$$\Delta\theta = \frac{L\cos\theta}{r} = \frac{L\cos^2\theta}{h} \tag{4-11}$$

The equation derived for the doppler frequency shift contained along the distance L was

$$\Delta f_d = \frac{2vf}{c}\cos\theta\,\Delta\theta \tag{4-12}$$

Substituting $\Delta\theta$, the doppler shift equation becomes

$$\Delta f_d = \frac{2 v f L}{c h} \cos^3 \theta \qquad (4\text{-}13)$$

It is necessary to have an equation of L as a function of other parameters This is obtained by rearranging the doppler frequency shift equation to obtain the following

$$L = \frac{\Delta f_d h c}{2 v f \cos^3 \theta} \qquad (4\text{-}14)$$

where all parameters are as previously defined

A value for L is necessary to solve for the frequency change, Δf_c, necessary to afford signal independence between signals of different frequencies. Substituting L into this equation will constitute the final step in the derivation of the Δf_c equation Thus,

$$\Delta f_c = \frac{c}{2 L \sin\theta} = \frac{v \cos^3 \theta}{h \Delta f_d \sin\theta} f \qquad (4\text{-}15)$$

This is only an approximation which tends to hold as $\Delta\theta$ becomes small.

Consider the case where extreme conditions for a scatterometer viewing from an aircraft are

maximum aircraft velocity, v = 150 m/sec
minimum aircraft height, h = 600 m
minimum Δf_d = 280 Hz
$\theta = 50°$
frequency, f = 13 3 GHz

The necessary frequency change, Δf_c, needed to afford signal independence becomes, with substitution of the given parameter values

$$\Delta f_c = \frac{(150)(.6425)}{(600)(280)(.766)} 13.3 \times 10^9$$

$$= 4.11 \times 10^6$$

$$= 4.11 \text{ MHz}$$

Thus, for the extreme conditions stated, a frequency change of 5 MHz implemented between pulse to pulse transmission will assure that the reflected pulses will be independent.

Previous work has centered on applying all techniques to a scatterometer having a transmission frequency of 13.3 GHz For this scatterometer, transmission for 0 2 seconds and reception from a ground area delineated

by a doppler frequency change of 280 Hz in the flight direction caused 18 independent samples to be received This number of independent samples came as a result of a monochromatic transmission. Suppose the scatterometer transmission frequency is increased by Δf_c = 5 MHz from pulse to pulse for twenty consecutive pulses and then repeated. This corresponds to using M = 20 in Fig. IV-1. The number of independent samples using this frequency agility would be twenty times the number arrived at using the monochromatic signal For the above mentioned transmission and reception specifications, at least 20 x 18 = 360 independent samples would be received. This is dependent upon the requirement that the extreme conditions used to calculate Δf_c will be applied to the scatterometer.

In using a frequency variation, the equation for the backscatter coefficient will have an inherent error, as stated before, due to its calculation by the scatterometer's data normalizer being dependent upon a specific wavelength or frequency value. The backscatter coefficient, σ_0, can be considered as a function of either $\frac{1}{\lambda^3}$ or f^3. The variance in σ_0 is calculated as follows

$$\pm \delta \sigma_o = 1 - \left(1 + \frac{\delta f}{f}\right)^3$$

$$= 1 - \left(1 + \frac{.5}{133}\right)^3$$

$$= .01$$

in db, this will be

$$\delta \sigma_o = \pm 10 \log 1.01$$

$$= \pm .04 \text{ db}$$

Thus, for the case cited, in causing an inherent db variance of ±.04 db in the calculated value of σ_0, the number of independent samples are increased from 18 to 20 x 18 or 360. The use of frequency agility must then be considered to be advantageous from the standpoint of the ability to increase the number of independent samples with only a small inherent error in σ_0.

CHAPTER V

CONCLUSION

A system analysis was performed to determine the effectiveness and accuracy of measuring backscatter coefficient for a proposed scanning radar scatterometer. The scatterometer system was examined in detail by individual subassemblies transmission, reception, signal reduction and logic, recording, and CRT display The system calibration and klystron operations were presented and analyzed in regards to implementation effectiveness and to transmission frequency drift respectively The possibility of improper CRT display of the obtained backscatter coefficient values was presented, and a method for correcting the problem is suggested.

Although the problems of transmission frequency drift and improper CRT display illumination were shown to be either inconsequencial or easily resolved, the problem of calibration presented some difficulty By mixing the calibration and intermediate frequency signals of equal amplitude with the return signal spectrum, improper power distribution was shown to occur. Equipment capable of handling a calibration signal of amplitude much smaller than the intermediate frequency signal amplitude could possibly solve this situation, but efforts must be made

to assure that the calibration signal amplitude is greater than any system noise level An alternate effective method for injecting the calibration signal into the scatterometer system was presented.

The accuracy of the mean determinance of a backscatter signal using a half-wave linear detector was analyzed. The analysis was conducted such that all results are applicable to the proposed scatterometer system. Since the accuracy of a stochastic signal process must be defined in terms of signal independence, an autocorrelation function was derived which describes signal independence and is applicable to the scatterometer system The mean value of the input signal was assumed to be zero in order to derive the autocorrelation function. This being a necessary, but incorrect, assumption, stringent specifications as to what constitutes signal independence were defined for the autocorrelation function The scatterometer reception of the Rayleigh distributed voltage return signal was shown to contain 18 independent samples during the 0 2 second integration time for a doppler bandwidth of 280 Hz. Averaging 18 independent samples gave a level of confidence of 73% that the backscatter coefficient is correct to within ±1 0 db of the true value These results are considered inadequate, an adequate level of confidence being considered greater

than 90%. It was shown that adequate results can be obtained by averaging at least 49 independent samples This increase in independent samples can be obtained by either increasing the doppler bandwidth or the viewing time for a terrain cell. Since the minimum doppler frequency used in defining a terrain cell size is utilized to determine the number of independent samples, the accuracy of the calculated backscatter coefficient for this cell can be considered the worst case.

The advantages of implementing frequency agility in the transmission section of the scatterometer were derived utilizing a specified frequency autocorrelation function. The number of independent sample was shown to greatly increase by utilizing frequency agility The use of frequency agility in the scatterometer was deemed advantageous from the standpoint of improving the accuracy of the backscatter coefficient determinance. The main disadvantage incurred utilizing frequency agility is that of increased hardware complexity.

In order to increase the scatterometer accuracy without increasing the original integration time and terrain cell size, the effects of utilizing a frequency agility transmission system were investigated. Using a specified frequency autocorrelation, the implemented frequency change necessary to gain pulse-to-pulse signal

independence was found to be about 5 MHz An example, using the proposed scatterometer specifications, showed that the utilization of frequency agility was very advantageous from the standpoint of accuracy

The frequency autocorrelation utilized is a function of target length and not target roughness A frequency autocorrelation function dependent upon the surface decorrelation distance has been attempted [33] Further work dealing with frequency autocorrelation functions for rough surfaces is justified and necessary before any implementation of frequency agility in the field of scanning radar scatterometers

It is believed that future derivations concerning frequency autocorrelation functions should relate the critical frequency change and the surface decorrelation distance as directly proportional Thus, the rougher the surface, the smaller the frequency change Exactly how this function will appear is as yet uncertain, but its derivation could be a major factor in the design of future scatterometer systems

BIBLIOGRAPHY

[1] Useful Applications of Earth-Oriented Satellites, National Academy of Sciences, Washington, D. C , 1969.

[2] R. K Moore, "Radar as a Sensor," University of Kansas, Lawrence, CRES Rept. 61-7, 1966

[3] P Beckmann and A Spizzichino, The Scattering of Electromagnetic Waves from Rough Surfaces New York The MacMillan Co., 1963, p. 119

[4] J. Rouse, Jr., H. MacDonald, and W Waite, "Geoscience Applications of Radar Sensors," IEEE Transactions on Geoscience Electronics, vol. GE-7, pp 2-19, January 1969.

[5] R. K Moore, "Radar Scatterometry - An Active Remote Sensing Tool," University of Kansas, Lawrence, CRES Rept 61-11, 1966

[6] J W Rouse, Jr , "Arctic Ice Type Identification Radar," Proc. IEEE, vol. 57, pp 605-611, April 1969.

[7] R W Newton, "Radar Scatterometer Data Analysis Sea State," Texas A&M University, College Station, Tech. Rept. RSC-09, 1970.

[8] N Guinard and J Daley, "An Experimental Study of a Sea Clutter Model," Proc IEEE, vol. 58, pp. 543-550, April 1970.

[9] J W Rouse, Jr., "Radar Scatterometer Data Analysis," Texas A&M University, College Station, Tech Rept RSC-01, 1969

[10] J. W Rouse, Jr , "The Frequency Dependence of Backscatter from Rough Surfaces," University of Kansas, Lawrence, CRES Rept. 133-4, 1968

[11] W Ament, F MacDonald, and R Schewbridge, "Radar Terrain Reflections for Several Polarizations and Frequencies," Naval Research Laboratory, Unpublished Rept , 1959.

[12] R Cosgriff, W. Peake, and R Talor, "Terrain Scattering Properties for Sensor System Design," Ohio State University Engineering Experiment Station, Columbus, Bulletin No 29(3), 1960

[13] J Lundien, "Terrain Analysis by Electromagnetic Means," U S. Army Engineer Waterways Experiment Station, Tech. Rept No. 3-693, 1966

[14] D Earing, "Target Signature Analysis Center Data Compilation, Second Supplement," University of Michigan, Institute of Science and Technology, Ann Arbor, 1967.

[15] W Birkemeier and N. Wallace, "Radar Tracking Accuracy Improvement by Means of Pulse-to-Pulse Frequency Modulation," Trans AIEEE, vol 81, pp 571-575, 1962

[16] R E. Chapman, "Systems Specifications - Model 719 Scanning Scatterometer," Ryan Aeronautical Co , San Diego, Internal Report, 1969

[17] T K Ishii, Microwave Engineering. New York Ronald Press Co., 1966, p 231.

[18] R. E Chapman, op cit

[19] G W Dalke, J. E. Rathke, J W Rouse, Jr., "Initial Design Considerations for the Multi-Color Display," University of Kansas, Lawrence, CRES Tech. Memo 61-5, 1964.

[20] A Papoulis, Probability, Random Variables, and Stochastic Processes. New York McGraw Hill, 1965, p 100-104.

[21] R. E Chapman, op. cit.

[22] W Davenport, Jr and W Root, Random Signals and Noise. New York McGraw Hill, 1958, p 271

[23] Ibid., p 104

[24] A. Papoulis, op cit , p. 266

[25] A Papoulis, op. cit., pp 266-268.

[26] R. K. Moore, "Radar Scatterometry - An Active Remote Sensing Tool," ibid.

[27] A. Papoulis, op cit., p. 260

[28] A. Papoulis, op cit., p 94.

[29] A. Papoulis, op. cit., p. 64.

[30] A. Papoulis, op. cit., p. 129

[31] I. Katz, "Wavelength Dependence of the Radar Reflectivity of the Earth and Moon," J. Geophysical Research, vol. 71, pp. 361-366, Jan. 15, 1966

[32] W. Birkemier and N. Wallace, op. cit.

[33] R. Moore, W. Waite, J. Rouse, Jr., "Panchromatic and Polypanchromatic Radar," Proc. IEEE, vol. 57, pp. 590-593, April 1969.

VITA

Richard Harrison Arnold [redacted] the son of Mr. and Mrs Howard Harrison Arnold He received his elementary education at several schools and graduated from Lafayette High School, Lafayette, Louisiana, in May, 1965.

Mr. Arnold then attended the University of Southwestern Louisiana at Lafayette. He graduated with honor in May, 1969, having become a member of Eta Kappa Nu, Tau Beta Pi, and IEEE, and received the Bachelor of Science Degree in Electrical Engineering. During the 1968 summer secession, he was employed as a Student Change Engineer at The Boeing Co in New Orleans working with the Apollo Saturn V Boosters

In June, 1969, Mr Arnold entered Texas A&M University and completed the requirements for a Master of Science Degree in Electrical Engineering in August, 1970 During his tenure at Texas A&M University, he was employed as a Research Assistant by the Remote Sensing Center

Mr Arnold is married to the former Clara Elizabeth Rountree and has a daughter Grace Elizabeth He can be reached at P O. Box 468, Pineville, Louisiana, 71360

The typist for this thesis was Mrs. James Ronald Bush

The REMOTE SENSING CENTER was established by authority of the Board of Directors of the Texas A&M University System on February 27 1968 The CENTER is a consortium of four colleges of the University, Agriculture, Engineering Geosciences and Science. This unique organization concentrates on the development and utilization of remote sensing techniques and technology for a broad range of applications to the betterment of mankind.